

## Durham Research Online

---

### Deposited in DRO:

15 October 2019

### Version of attached file:

Published Version

### Peer-review status of attached file:

Peer-reviewed

### Citation for published item:

Davies, B.J. and Livingstone, S.J. and Roberts, D.H. and Evans, D.J.A. and Gheorghiu, D.M. and Ó Cofaigh, C. (2019) 'Dynamic ice stream retreat in the central sector of the last British-Irish Ice Sheet.', *Quaternary science reviews.*, 225 . p. 105989.

### Further information on publisher's website:

<https://doi.org/10.1016/j.quascirev.2019.105989>

### Publisher's copyright statement:

© 2019 The Authors. Published by Elsevier Ltd. This is an open access article under the CC BY-NC-ND license (<http://creativecommons.org/licenses/by-nc-nd/4.0/>)

### Additional information:

---

### Use policy

The full-text may be used and/or reproduced, and given to third parties in any format or medium, without prior permission or charge, for personal research or study, educational, or not-for-profit purposes provided that:

- a full bibliographic reference is made to the original source
- a [link](#) is made to the metadata record in DRO
- the full-text is not changed in any way

The full-text must not be sold in any format or medium without the formal permission of the copyright holders.

Please consult the [full DRO policy](#) for further details.



# Dynamic ice stream retreat in the central sector of the last British-Irish Ice Sheet

B.J. Davies <sup>a,\*</sup>, S.J. Livingstone <sup>b</sup>, D.H. Roberts <sup>c</sup>, D.J.A. Evans <sup>c</sup>, D.M. Gheorghiu <sup>d</sup>,  
C. Ó Cofaigh <sup>c</sup>

<sup>a</sup> Centre for Quaternary Research, Department of Geography, Royal Holloway University of London, Egham, Surrey, TW20 0EX, UK

<sup>b</sup> Department of Geography, University of Sheffield, Sheffield, S10 2TN, UK

<sup>c</sup> Department of Geography, Durham University, Science Laboratories, South Road, Durham, DH1 3LE, UK

<sup>d</sup> NERC Cosmogenic Isotope Analysis Facility, SUERC, Rankine Avenue, East Kilbride, G75 0QF, UK

## ARTICLE INFO

### Article history:

Received 4 June 2019

Received in revised form

1 September 2019

Accepted 3 October 2019

Available online xxx

### Keywords:

Quaternary

Glaciation

Western Europe

Geomorphology

Glacial

Cosmogenic isotopes

## ABSTRACT

During the Last Glacial Maximum (LGM), ice streams of the last British-Irish Ice Sheet (BIIS) controlled ice discharge from various dispersal centres. Deglaciation was characterised by shifts in ice-divide location and changes in internal ice-sheet dynamics, resulting in substantial flow switches and significant ice-stream reconfiguration, and hence modification of their landform signatures. We present new geomorphological mapping and  $^{11}\text{Be}$  cosmogenic nuclide ages from Northern England (Stainmore Gap, Eden Valley and Vale of York), that constrain regional dynamic ice-stream retreat following the LGM. We identify complex decoupling of competing ice lobes, characterised by early retreat of the North Sea Lobe and a minor re-advance of Stainmore ice prior to  $\sim 20$  ka. This was followed by rapid recession of the central Stainmore Gap, which was ice-free by  $19.8 \pm 0.7$  to  $18.0 \pm 0.5$  ka, contemporaneous with the recession of the Tyne Gap Ice Stream. In the southern Vale of Eden, Crossby Ravensworth Fell became exposed between 19.2 and 20.3 ka. The northwards ice-flow reversal in the Vale of Eden was associated with the development of ice domes across the northern Pennines, Howgill Fells and the Lake District. This shift in dispersal centres and ice divide migration likely triggered the rapid collapse of eastward ice stream corridors. The central sector of the BIIS rapidly collapsed back up into upland dispersal centres between 20 and 17.5 ka. This work highlights the role internal factors, such as topography, in driving ice-divide migration and flow switches during externally and climatically forced ice-sheet thinning.

© 2019 The Authors. Published by Elsevier Ltd. This is an open access article under the CC BY-NC-ND license (<http://creativecommons.org/licenses/by-nc-nd/4.0/>).

## 1. Introduction

Ice streams exert an important influence on ice-sheet geometry, mass balance and stability (Bamber et al., 2000; Stokes and Clark, 2001; Bennett, 2003; Rignot et al., 2011). Palaeo ice stream reconstructions provide an important context for assessing recent and future changes in contemporary ice streams, and for investigating controls underlying their behaviour (Stokes et al., 2015). The last British-Irish Ice Sheet (BIIS) was drained by ice streams that were dynamically variable through time and space (Hubbard et al., 2009; Evans et al., 2009). These ice streams were sensitive to changes in ice divide location driven by external climatic and oceanographic forcing (Clark et al., 2012; Livingstone et al., 2012).

Upland ice dispersal centres such as the Cheviots, Southern Uplands, Lake District and Pennines (see Fig. 1) played an important role in seeding and modulating ice flow and controlling the major ice stream locations. This is reflected in the geological record, which indicates complex, multi-phase ice flow behaviour and repeated marginal fluctuations of the Stainmore-Eden, Tyne Gap, Tweed, North Sea Lobe and Firth of Forth ice streams (Fig. 1).

Although there is a wealth of geomorphological and sedimentological evidence constraining former ice-sheet flow in the central sector of the BIIS during the LGM (Clapperton, 1970; Evans et al., 2009, 2018; Livingstone et al., 2008, 2010b, 2010c, 2010d, 2010e, 2012, 2015; Evans and Thomson, 2010; Stone et al., 2010; Davies et al., 2009, 2011, 2012, 2013; Clark et al., 2012, 2018; Hughes et al., 2014; Boston et al., 2010), the timing and rate of retreat is poorly constrained, particularly through the Eden valley and Stainmore Gap, which routed a major ice stream across the central UK. In the Stainmore valley region, there is only a single basal

\* Corresponding author.

E-mail address: [bethan.davies@rhul.ac.uk](mailto:bethan.davies@rhul.ac.uk) (B.J. Davies).

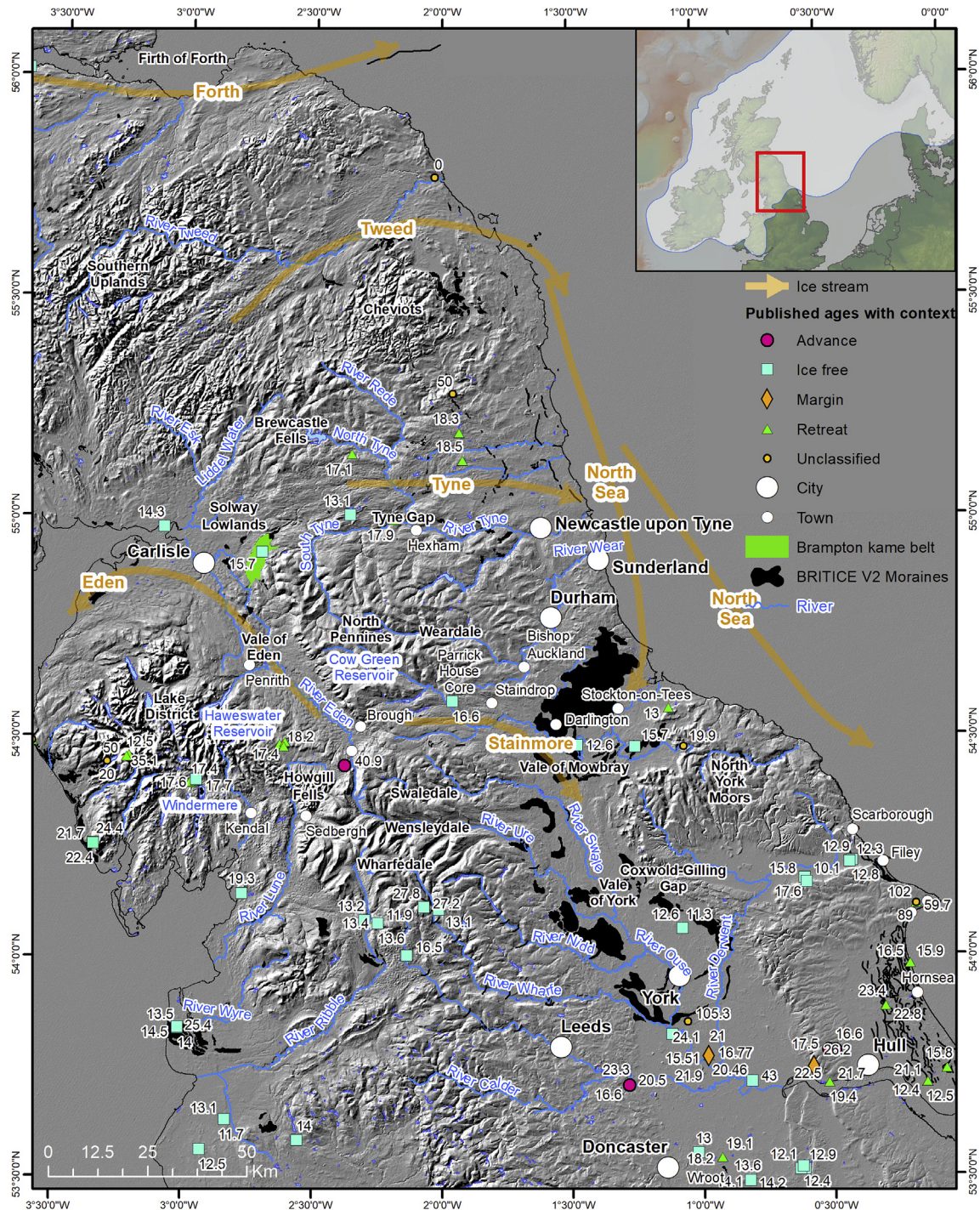


**Fig. 1.** Key locations and ice streams (orange arrows) of the central sector of the last British-Irish Ice Sheet. Published ages and geomorphology are shown (Bateman et al., 2015; Hughes et al., 2011, 2016; Chiverrell et al., 2018; Lovell et al., 2019; Wilson et al., 2013a; Livingstone et al., 2015; Innes and Evans, 2017). Note the absence of ages in the Stainmore and Eden valleys. Overlain on a hillshaded SRTM DEM. Inset shows 'most credible' ice-sheet extent at 27 ka from the DATED-1 database (Hughes et al., 2016). Cosmogenic nuclide ages have been recalculated following the protocols outlined in the Methods section. (For interpretation of the references to colour in this figure legend, the reader is referred to the Web version of this article.)

radiocarbon age of 16.6 ka cal. BP from Parrick House in upper Teesdale (Fig. 1) (Innes and Evans, 2017), highlighting the dearth of chronological information in this area. Furthermore, the Vale of Eden purportedly preserves geomorphological evidence of a major reversal of ice flow by 180° close to the centre of the ice sheet (Rose and Letzer, 1977). However, the dating and palaeoglaciological controls on this reorganisation remain poorly understood, thereby

limiting our knowledge of ice-ocean-atmosphere interactions and external climatic controls on BIIS behaviour. In addition, the interaction and switch in dominance between the east-coast North Sea Lobe, which penetrated into the Vale of York from the east, and the Eden-Stainmore Ice Stream, which flowed into the Vale of York from the west, is also poorly understood, due to a lack of detailed geomorphological mapping of moraines and limited direct dating



of landforms (Fig. 1; cf. Blackburn, 1952; Plater et al., 2000; Clark et al., 2004, 2018; Evans et al., 2005). As a result, the complex interplay between ice stream operation, ice divide and related ice-flow pathway changes, and the drivers of regionally variable rates of recession, are poorly known, despite this central region being key to our understanding of the dynamics of the BIIS as a whole. A critical question is whether deglaciation of the ice streams draining eastwards from the BIIS into the North Sea Basin (Eden-Stainmore, Tyne, Tweed, Forth) were controlled by external climatic factors, or whether deglaciation was asynchronous and controlled by internal factors such as topography, subglacial conditions such as lubrication and meltwater, and ice-divide migration during thinning. To explore this challenging question, more detail on the timing and nature of ice-stream recession is needed.

This study aims to determine the nature and timing of deglaciation in the Vale of York, Vale of Mowbray, Eden and Stainmore valleys (Fig. 1), and to relate these findings to the regional patterns of BIIS deglaciation. These data provide insights into broader controls on changes in palaeo ice-stream dynamics, changing ice divides, and shifts in centres of ice dispersal of the last BIIS. We present new geomorphological mapping (focusing on marginal meltwater channels and moraines) and 11 new  $^{10}\text{Be}$  cosmogenic nuclide ages from the Stainmore Gap and Eden Valley. This facilitates the dating of flow-sets and ice marginal positions and provides new temporal constraints on the ice-flow phasing (synchronicity) of the Eden-Stainmore Ice Stream and the North Sea Lobe.

## 2. Study area

### 2.1. Physiography and geology

The area covered by the former central sector of the last BIIS has a complex physiography, with three geologically controlled upland regions: the Alston Block (comprising northern Pennines, the Yorkshire Dales and Howgill Fells), the Lake District, the Southern Uplands, the Tyne Gap and the Solway Lowlands (Fig. 1). The Alston Block forms the highest terrain in the north Pennine hills, but several table-like high elevation plateaux occur further south (e.g. Howgill Fells, Wild Boar Fell, Baugh Fell; Fig. 2), reaching heights of over 700 m asl (Evans et al., 2018). The Alston Block comprises Carboniferous rocks, including limestones, shales, sandstone and Millstone Grit and Westphalian Coal Measures, dipping gently eastwards (Johnson, 1995; Aitkenhead et al., 2002; Stone et al., 2010). Regional glacial landforms commonly display strong bedrock control, with streamlined bedforms, valley-side benches, flat-topped mountain summits and buttes all reflecting the flat-lying to shallow dipping Carboniferous strata (Evans, 2017). In the northern Pennines and Teesdale, the local bedrock structure has formed an eastward dipping dissected plateau (King, 1976; Mills and Hull, 1976; Evans et al., 2018). West of Middleton-in-Teesdale (Fig. 2), the Teesdale valley is aligned with the Teesdale Fault, and therefore forms a deep incision in the sub-horizontally bedded Carboniferous Limestones. Further south, the Yorkshire Dales also comprise Carboniferous rock, but to the west, the Howgill Fells are of Ordovician and Silurian age, and are predominantly composed of Conistone Grit.

The Tyne Gap and Stainmore Gap are large topographic lows that cut through the upland chain of the Pennine hills. The Tyne Gap constitutes a transection-type valley (cf. Linton, 1962), and was the route-way for an easterly flowing ice stream during the last glaciation (Livingstone et al., 2015). The glacial signature of the Tyne Gap Ice Stream is strongly influenced by the geological structure, which consists of SSE dipping Carboniferous sedimentary rocks intruded in places by the resistant strata of the Whin Sill

dolerite.

The Stainmore Gap contains a high col at 533 m (Fig. 2) and is dissected by valleys only to the east of the Pennine watershed. It acted as a major conduit of ice flow through the Pennines (Catt, 1991), allowing the Eden-Stainmore Ice Stream to flow eastwards towards Yorkshire and the North Sea (Mitchell and Riley, 2006). Glacial landforms in the valleys include drumlins and subglacial lineations, eskers, meltwater channels and glaciofluvial deposits (Livingstone et al., 2010a; Evans et al., 2018).

Another important area is the Vale of Eden, which is a north-west/southeast trending valley that opens and broadens into the low-lying (<100 m) coastal plain of the Solway Lowlands. It is bounded at its southern, western and eastern margins by the upland terrains of the Howgill Fells, Lake District and northern Pennines respectively. It is floored by Permo-Triassic rocks, which are predominantly sandstone.

The Vale of York is a broad, low-lying area of gently undulating land in northeast England, constrained between the Jurassic and Cretaceous rocks of the Yorkshire Wolds to the east and the Permian and Carboniferous rocks of the Pennines to the west. It is underlain by Triassic sandstones and mudstones (Straw and Clayton, 1979; Hall et al., 2010). Superficial deposits here include till, glaciofluvial sands and gravels and glaciolacustrine clays, all covered to varying extents and depths by peat and alluvium (Cooper and Burgess, 1993). The Vale of Mowbray sits at the northern end of the Vale of York and is underlain by Triassic and Permian rocks with overlying till and glaciofluvial sediments.

### 2.2. Regional glacial history

The geomorphic footprint of ice streams in the central sector of the last BIIS has been well documented, with glacial bedforms (largely drumlins) used to generate flowsets to reconstruct ice flow changes through time (Livingstone et al., 2008, 2012) (Figs. 2–4). Meltwater channels (Fig. 3c) have been mapped by multiple authors (Mills and Hull, 1976; Arthurton and Wadge, 1981; Greenwood et al., 2007; Hughes, 2008; Livingstone et al., 2008, 2010c; Evans et al., 2018). The meltwater channels of Teesdale record the earliest stages of Stainmore ice downwasting and recession as a partially topographically-confined lobe (Evans et al., 2018). However, few meltwater channels are mapped in the central Stainmore valley, Weardale, Swaledale, Wensleydale, the Vale of Mowbray or the Vale of York.

Ice flow through the Stainmore Gap created drumlins across the floor of Stainmore (Fig. 3) and deposited the Stainmore Forest Till Formation, which contains local Carboniferous lithologies and Lake District erratics including Shap granite (Stone et al., 2010; McMillan et al., 2011). Flowsets ST1 and 2 and ES1 are associated with the “Main Glaciation” (23–29 cal ka BP) (Table 1; Livingstone et al., 2012). During this time (“Local Last Glacial Maximum” (LLGM; 27 cal ka BP)), ice flowed eastwards across the Pennines, through the Tyne and Stainmore gaps (Fig. 4A), forming the Tyne Ice Stream and Eden-Stainmore Ice Stream (Davies et al., 2009; Livingstone et al., 2008; Evans et al., 2009; Hughes et al., 2016).

The Eden-Stainmore Ice Stream drained into the Vale of York (ST1; Gaunt, 1975; Boulton et al., 1985; Bateman et al., 2015). Together, the 125 km long Vale of York Lobe and the North Sea Lobe dammed Glacial Lake Humber in the Vale of York (Fig. 4) (Edwards, 1937; Dalton, 1941; Gaunt, 1974; Murton et al., 2009; Fairburn and Bateman, 2016; Bateman et al., 2015, 2018). Glacial Lake Humber continued to exist until around  $13.7 \pm 0.4$  ka, likely dammed by moraines, with lake levels progressively dropping over the several thousand years prior to complete drainage (Bateman et al., 2015, 2018; Fairburn and Bateman, 2016).

The North Sea Lobe (Flowset EC-1) also dammed Glacial Lake



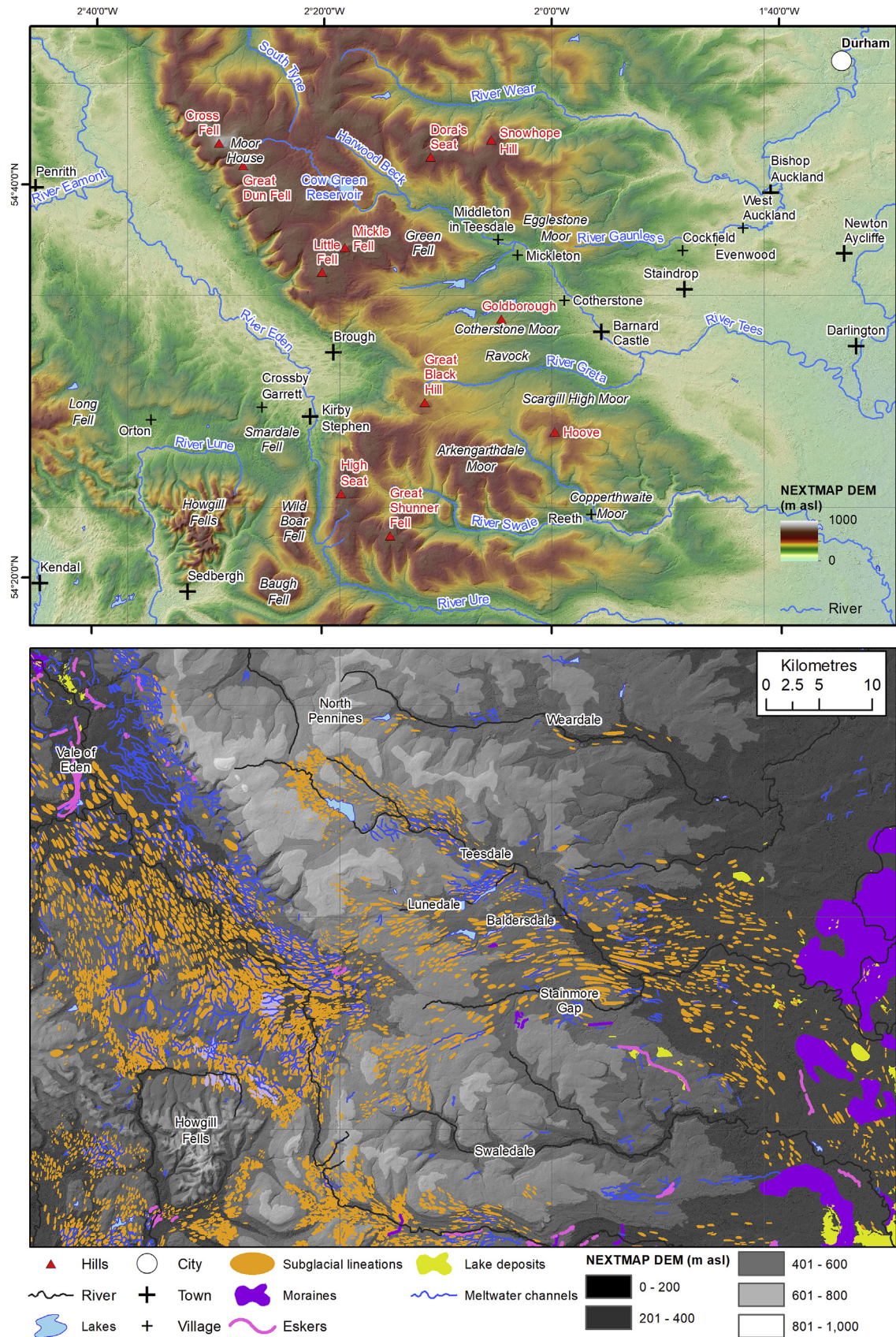


**Fig. 2.** A. Study area and place names mentioned in text. B. Drumlins, moraines and meltwater channels mapped across the study area from the BRITICE V2 database (Clark et al., 2018). Scale bar applies to both map panels. Grid spacing = 20 km.



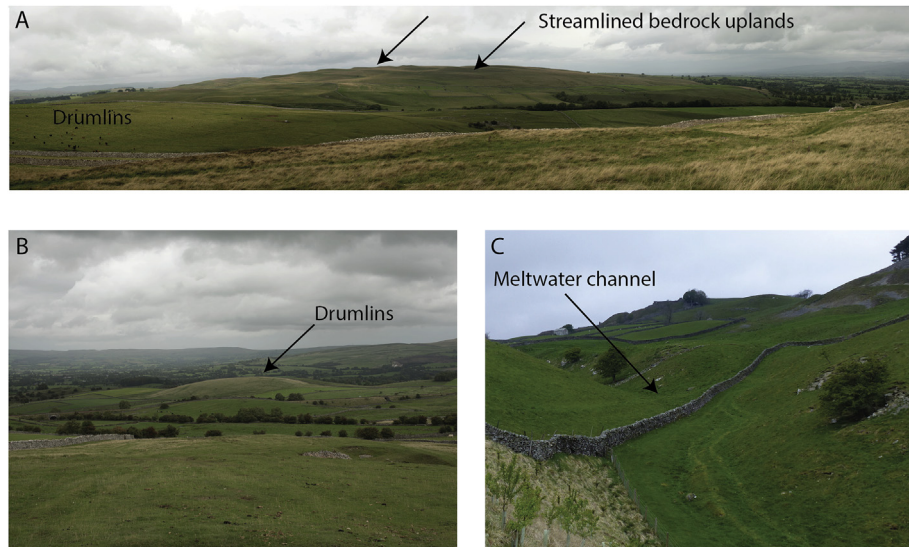


**Fig. 3.** A: Streamlined bedrock on uplands around Smardale Fell, Vale of Eden, Southwest of Kirby Stephen, with drumlins in the foreground. B: Drumlins around Smardale. C: Lateral meltwater channel in the interfluve area between Teesdale and Stainmore.

Pickering in the North York Moors (Evans et al., 2017a), which was also dammed by the Vale of York Lobe at the Cotswold-Gilling Gap (Figs. 1 and 4). Glacial Lake Humber formed in the Vale of York (Edwards, 1937; Dalton, 1941; Gaunt, 1974; Fairburn and Bateman, 2016; Bateman et al., 2018), dammed by the North Sea Lobe in the Humber Gap. Glacial Lake Tees formed in the lowlands at the mouth of the River Tees (Plater et al., 2000), and Glacial Lake Wear formed in County Durham (Murton and Murton, 2012) (Fig. 4). Optically Stimulated Luminescence (OSL) ages from Holderness indicate that the western limit of the North Sea Lobe in this area was reached at c. 21.6 ka (Bateman et al., 2018) (Fig. 1). The North Sea Lobe advanced to north Norfolk as early as 30–25 ka, then underwent a retreat to the north of Dogger Bank at ca. 23 ka, before re-advancing to the Norfolk coast 22–21 ka. Recession of the North Sea Lobe northwards was accompanied by sporadic marginal oscillations, but the ice was north of the Tees by 19 ka (Roberts et al., 2018a).

Migration of ice divides back towards upland massifs meant that drainage through the Tyne and Stainmore gaps diminished, resulting in flowsets LT4 down the North Tyne and ST3 to 4 out of Teesdale (Livingstone et al., 2012).  $^{10}\text{Be}$  cosmogenic exposure ages from the Tyne Gap indicate deglaciation of the Tyne Gap Ice Stream by 18.7 to 17.1 ka (Livingstone et al., 2015). This may be related to the expansion of the Southern Uplands-Scottish Highlands ice divide (Finlayson et al., 2010; Livingstone et al., 2015), and increased topographic focusing of ice flow and thinning during deglaciation (Hughes et al., 2014).

There is prominent streamlining on the floor of Teesdale, in the Stainmore Gap and in the Lunedale and Baldersdale valleys (Fig. 2) (Clark et al., 2018; Evans et al., 2018). Large glaciers in Teesdale (ST3 and ST4 in Fig. 4) and Weardale contributed to easterly regional ice flow during the last glaciation (Evans et al., 2018), but the ice in these valleys was more topographically confined than the larger ice streams in the Tyne Gap and Eden-Stainmore Gap. The suture zone between Teesdale and Eden-Stainmore ice is delineated by the maximum northern limit of Shap granites carried across from the Lake District by Stainmore ice (Harmer, 1928; Evans et al., 2017b). The “Cockfield Moraine” (near Cockfield; cf. Fig. 2) cross-cuts drumlins created by the Eden-Stainmore Ice Stream (Evans et al., 2018), and represents the southernmost extension of the Teesdale ice margin when it decoupled from Eden-Stainmore ice to the east

and northeast of Barnard Castle.

The geomorphic record of the Vale of Eden supports two separate flowsets (Fig. 4); an earlier stage with ice converging into Stainmore from the north, west and south, forming a significant ice stream that extended into eastern England and the Vale of York (ST1, ST2), and a later stage dominated by ice flowing northwards down the Vale of Eden into the Solway Lowlands (LT6) (Rose and Letzer, 1977; Mitchell and Riley, 2006). This ice-flow reversal may have occurred due to the development of an ice divide orientated west to east from the Lake District through the Howgill Fells and on to Arkengarthdale Moor (Mitchell, 1994; Mitchell and Riley, 2006; Mitchell et al., 2010), and resulted in ice draining west towards the Irish Sea Basin (LT5) as a tributary of the Irish Sea Ice Stream (Stone et al., 2010).

The LT6 flow phase in the Vale of Eden records the final re-advance of ice into the Solway Lowlands, and may have been coeval with the Scottish Re-advance into the northern Solway Lowlands (Livingstone et al., 2010b), although dating constraints are limited. The Scottish Re-advance (SF1; Fig. 4) is thought to have been the final incursion of Scottish ice into the Solway Lowlands and Irish Sea (Trotter and Hollingworth, 1932; Huddart et al., 1977; Livingstone et al., 2010b; Chiverrell et al., 2018). Ages constrain the deglaciation of Cumbria following the Scottish Re-advance to 19.2–18.2 ka (Chiverrell et al., 2018). This phase of ice flow is associated with the development of the Brampton Kame Belt (Lovell et al., 2019, Figs. 1 and 4), which comprises a substantial glacio-fluvial depositional zone in the Solway Lowlands. The Brampton Kame Belt includes a series of fragmented SW-NE aligned esker ridges that document recession of the Vale of Eden ice lobe south-eastwards up the Vale of Eden. This was followed by final retreat into upland dispersal centres, with a small ice cap in the Lake District (flowset LT7; Fig. 4), and potentially a plateau icefield over the northern Pennines (Evans et al., 2018).

Moraines relating to ice sheet recession across the North Pennines have not been widely mapped in previous studies (see Clark et al., 2004 and Evans et al., 2005 for reviews). Evidence of the interaction between the North Sea Lobe and Eden-Stainmore Ice Stream is in particular poorly documented, with few moraines recording recession of Stainmore ice from the Vale of Mowbray. The separation of ice in the Vale of York from ice in Swaledale and Wensleydale (Fig. 4) is also poorly constrained. Gaps in

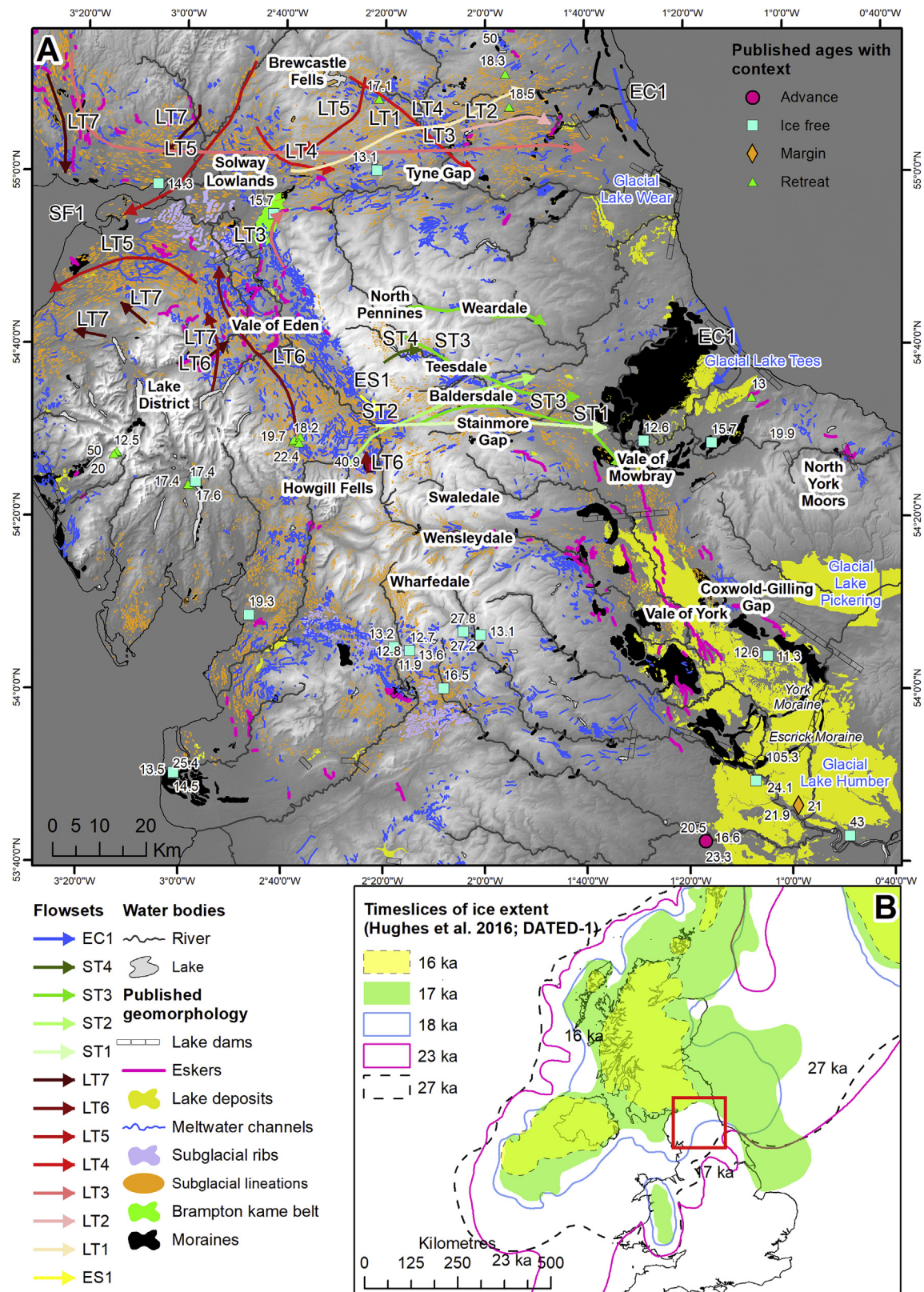


**Fig. 4.** A. Published geomorphology and ages of the central sector of the British-Irish Ice Sheet. Note the absence of ages and limited mapping, except for glacial lineations, in the Stainmore Gap. Geomorphology taken from the BRITICE V2 database (Clark et al., 2018) and, in Teesdale, from Evans et al. (2018). Brampton Kame Belt from Lovell et al. (2019). Published ages compiled by Hughes et al. (2011, 2016) with addition of newly published ages (Wilson et al., 2013a; Livingstone et al., 2015; Bateman et al., 2015, 2018). Cosmogenic nuclide ages have been recalculated according to the protocols of this paper (Methods). Flowsets are from Livingstone et al. (2008, 2012). Flowsets are arranged oldest at the bottom (e.g. LT1) to youngest at the top (e.g. LT7). Eight flow phases are identified within the Lake District-Tyne Gap region (LT). Four flow phases are recognised in the Stainmore (ST) region, and one in the East Coast (EC) region. Basemap is hillshaded NEXTMAP DEM. Only major rivers are shown. B. Regional ice-sheet view with timeslices (most credible) from Hughes et al. (2016). Note the readvance of the North Sea Lobe at 17 ka, and the major extent of the Irish Sea Ice Stream at 23 ka. Local LGM is at 27 ka.



**Table 1**

Description and location of cosmogenic nuclide samples. Ages were calculated in the CRONUS-Earth online calculators version 2.3 (Balco et al., 2008). Elevation/pressure flag is 'std'.  $^{10}\text{Be}$  standardisation is NIST\_27900. †Refers to stone shape, using Powers (1953) system for describing edge rounding. Calculated boulder exposure ages are given in Table 2.

Sample	Latitude	Longitude	Elevation (m asl)	Rock type	Boulder dimensions (L-W-H) (m)	Sample Density	Shielding correction	Sample position	Surface dip & direction (mag)	Evidence of glacial erosion†	$^{10}\text{Be}$ at/g Qtz	Processed blank ratio
S02	54.48717	-2.581499	369	Shap granite	1 × 0.7 × 0.8	2.7	0.9916	Upper surface of erratic	302/22	SA-SR, faceted, erratic	97051 ± 2637	4.85 × 10 <sup>-15</sup>
S03	54.4892	-2.587767	339	Shap granite	1.6 × 1.4 × 0.9	2.7	0.9975	Upper flat surface away from joints and cracks	185/06	SA-SR erratic	119359 ± 3558	4.85 × 10 <sup>-15</sup>
S04	54.4851	-2.588967	349	Shap granite	1.1 × 1.1 × 1.4	2.7	0.9973	Upper surface of erratic	350/02	SA-SR, faceted, erratic (SR-R on top)	130545 ± 3752	4.85 × 10 <sup>-15</sup>
S05	54.54068	-2.006968	313	Carboniferous Sandstone	Bedrock sample	2.6	0.9996	Upper surface of raised bedrock crag	330/08	Streamlined glacial landscape; glacially abraded	92726 ± 2282	4.85 × 10 <sup>-15</sup>
S06	54.54073	-2.007834	310	Carboniferous Sandstone	Bedrock sample	2.6	0.7219	Upper surface of raised bedrock crag	116/70	Streamlined glacial landscape; glacially abraded	94448 ± 2330	4.85 × 10 <sup>-15</sup>
S07	54.55463	-2.071783	391	Shap granite	1.6 × 1.5 × 1.8	2.7	0.9995	Upper surface of erratic	023/03	SA-SR erratic	100467 ± 2334	3.65 × 10 <sup>-15</sup>
S08	54.55473	-2.071083	388	Carboniferous Sandstone	Bedrock sample	2.7	0.9999	Flat top of outcrop on Monadnock	346/04	Streamlined glacial landscape	94795 ± 2460	4.85 × 10 <sup>-15</sup>
S09	54.55675	-2.075017	337	Shap granite	1.5 × 1.0 × 0.5	2.7	0.9995	Upper flat surface of erratic	0/0	SA-SR erratic	115453 ± 2852	3.65 × 10 <sup>-15</sup>
S10	54.63082	-1.978683	422	Sandstone, gritstone	1.0 × 1.0 × 0.5	2.6	0.9995	Upper flat surface of erratic	040/06	SA-SR erratic; adjacent to large meltwater channel	205999 ± 4336	4.85 × 10 <sup>-15</sup>
S11	54.63012	-1.986517	416	Carboniferous Sandstone	Bedrock sample	2.7	0.9999	Centre of flat-topped exposed bedrock crag	068/05	Onset zone of shallow meltwater channel	148065 ± 3213	4.85 × 10 <sup>-15</sup>
S12	54.62812	-1.996283	385	Sandstone	1 × 1.3 × 0.4	2.7	0.998	Upper surface of erratic	008/14	SA-SR erratic	106229 ± 2650	4.85 × 10 <sup>-15</sup>

understanding include: (1) the timing and dynamics of the separation of the ice masses in the valleys of the Pennines from the North Sea Lobe in the Vale of York and Vale of Mowbray; and (2) the controls on ice divide location that are critical in initiating the flow switch from ice flowing across the Stainmore Gap to ice flowing northwards through the Vale of Eden and into the Solway Lowlands.

### 3. Methods

#### 3.1. Geomorphological mapping

Geomorphological mapping utilised the 5 m resolution NEXT-Map dataset (<https://www.intermap.com/nextmap>) for England and Wales (cf. Hall et al., 2010) in a Geographic Information System (GIS), together with field surveys for ground checking landform interpretations. Key valleys were studied using hillshaded 1 m spatial resolution LiDAR (Light Detection and Ranging) digital surface model (DSM) (<https://data.gov.uk/dataset/lidar-composite-dtm-1m1>). Data were visualised using two orthogonal hillshades and slope raster images to assist with landform identification and to avoid azimuth bias (cf. Smith and Clark, 2005; Hughes et al., 2010; Hall et al., 2010).

Landforms were identified with reference to published criteria (Evans et al., 2005; Greenwood et al., 2007; Livingstone et al., 2008). As drumlins have already been comprehensively mapped in this region by other researchers (e.g. Mitchell and Riley, 2006; Livingstone et al., 2008; Hughes et al., 2010; Mitchell et al., 2010; Livingstone et al., 2010d; Clark et al., 2018; Evans et al., 2018),

mapping focused on meltwater channels and moraines, which have previously been mapped and classified in only localised detail (cf. Fig. 4).

Initial geomorphic mapping was conducted 'blind', without reference to previously mapped geomorphology, to avoid interpretive bias. Mapping was then checked against previously published datasets. The British Geological Survey 1:620,000 Superficial Deposits map (ESRI Shapefile) was used to cross-check identifications of sediment accumulations versus bedrock-controlled highs (DiGMapGB-625).

#### 3.2. $^{10}\text{Be}$ cosmogenic nuclide dating

Cosmogenic dating is widely used in glacial geology (Cockburn and Summerfield, 2004; Ivy-Ochs and Kober, 2007; Balco, 2011; Darvill, 2013). It can be used to date glacially transported boulders and exposed, eroded bedrock surfaces (Roberts et al., 2009; Corbett et al., 2011). In this study, we targeted samples along the central axis of the Stainmore Gap and across confluences with tributary glaciers. We sampled seven glacially transported boulders and four glacially abraded bedrock surfaces.

Sampling procedures recommended by Balco (2011) were followed, with erratic boulders sampled from flat upper surfaces, where there was no possibility of the boulder rolling, toppling, or sliding downslope. Bedrock samples were taken from exposed surfaces at the top of cliffs and scarps, where there was abundant regional evidence of glacial erosion. Samples were collected using a rock saw, allowing the removal of intact surface blocks (10 × 10 × 4 cm; ca. 3 kg) at least 30 cm from all edges, or hammer

**Table 2**

Calculated  $^{10}\text{Be}$  ages for the 11 new Stainmore cosmogenic nuclide samples and published samples using two different erosion rates and using the Loch Lomond Production Rate (LLPR). Ages calculated using a Global Production Rate (GPR) are included for comparison. Weighted mean ( $\mu_i \pm \sigma_i$ ) for samples from the same site is calculated using external uncertainties (in brackets) and the 0.0001 cm/yr erosion rate. Outliers, identified in Fig. 9, are indicated in italics and are not included in the weighted mean calculations. Sample locations shown in Fig. 5.

Location	Sample	AMS ID	LLPR $^{10}\text{Be}$ age Lal/Stone 0 cm/yr erosion rate	LLPR $^{10}\text{Be}$ age Lal/Stone 0.0001 cm/yr erosion rate	GPR $^{10}\text{Be}$ age Lal/Stone 0 cm/yr erosion rate	GPR $^{10}\text{Be}$ age Lal/Stone 0.0001 cm/yr erosion rate
Crosby Ravensworth Fell, north of Orton, Eastern Cumbria	S02	B10440	17164 $\pm$ 468 (885)	17414 $\pm$ 482 (911)	16739 $\pm$ 457 (1506)	16977 $\pm$ 470 (1550)
	S03	B10441	21611 $\pm$ 648 (1147)	22010 $\pm$ 672 (1190)	21075 $\pm$ 632 (1916)	21456 $\pm$ 655 (1986)
	S04	B10442	23429 $\pm$ 677 (1230)	23900 $\pm$ 705 (1280)	22849 $\pm$ 660 (2070)	23297 $\pm$ 687 (2153)
<b>Weighted mean</b>				<b>20270 <math>\pm</math> 630</b>		
Low Craggs, Stainmore Gap	S05	B10270	17127 $\pm$ 423 (861)	17368 $\pm$ 435 (885)	16704 $\pm$ 413 (1490)	16932 $\pm$ 424 (1532)
	S06	B10273	24125 $\pm$ 599 (1215)	24603 $\pm$ 623 (1264)	23530 $\pm$ 584 (2103)	23985 $\pm$ 607 (2187)
<b>Weighted mean</b>				<b>19750 <math>\pm</math> 730</b>		
Goldsborough Craggs, Stainmore Gap	S07	B10529	17265 $\pm$ 403 (856)	17519 $\pm$ 415 (882)	16837 $\pm$ 393 (1496)	17079 $\pm$ 404 (1540)
	S08	B10443	16325 $\pm$ 425 (831)	16552 $\pm$ 437 (855)	15921 $\pm$ 415 (1426)	16137 $\pm$ 426 (1466)
	S09	B10530	20901 $\pm$ 519 (1052)	21275 $\pm$ 538 (1091)	20384 $\pm$ 506 (1821)	20739 $\pm$ 524 (1885)
<b>Weighted mean</b>				<b>18040 <math>\pm</math> 540</b>		
Eggleston Moor, Teesdale	S10	B10274	34486 $\pm$ 732 (1683)	35483 $\pm$ 776 (1783)	33629 $\pm$ 714 (2982)	34576 $\pm$ 755 (3154)
	S11	BL0446	24887 $\pm$ 543 (1219)	25420 $\pm$ 567 (1272)	24270 $\pm$ 530 (2151)	24776 $\pm$ 552 (2243)
	S12	B10447	18383 $\pm$ 461 (927)	18671 $\pm$ 475 (957)	17928 $\pm$ 449 (1602)	18202 $\pm$ 463 (1651)
<b>Weighted mean</b>				<b>21110 <math>\pm</math> 770</b>		
Eastern Cumbria, west of Crossby Ravensworth Fell (Wilson et al., 2013a)	Shap-02	SUERCb5608	17965 $\pm$ 706 (1057)	18229 $\pm$ 727 (1088)	17521 $\pm$ 689 (1653)	17772 $\pm$ 709 (1701)
	Shap-03	SUERCb5610	19408 $\pm$ 673 (1084)	19720 $\pm$ 695 (1119)	18928 $\pm$ 656 (1751)	19225 $\pm$ 677 (1807)
	Shap-07	SUERCb5611	17199 $\pm$ 693 (1023)	17441 $\pm$ 713 (1053)	16773 $\pm$ 676 (1589)	17004 $\pm$ 695 (1633)
	Shap-08	SUERCb5612	21956 $\pm$ 793 (1246)	22354 $\pm$ 822 (1292)	21413 $\pm$ 773 (1994)	21790 $\pm$ 801 (2066)
<b>Weighted mean</b>				<b>19170 <math>\pm</math> 560</b>		
Eastern Tyne Gap (Livingstone et al., 2015)	TY01		18213 $\pm$ 688 (1053)	18490 $\pm$ 709 (1085)	17763 $\pm$ 671 (1664)	18026 $\pm$ 691 (1714)
	TY02		17989 $\pm$ 957 (1239)	18260 $\pm$ 986 (1277)	17545 $\pm$ 933 (1770)	17802 $\pm$ 961 (1823)
<b>Weighted mean</b>				<b>18390 <math>\pm</math> 830</b>		
Central Tyne Gap (Livingstone et al., 2015)	TY03		16818 $\pm$ 572 (932)	17054 $\pm$ 588 (958)	16403 $\pm$ 558 (1512)	16627 $\pm$ 573 (1555)
	TY04		47981 $\pm$ 1114 (2391)	49984 $\pm$ 1211 (2598)	46784 $\pm$ 1086 (4184)	48686 $\pm$ 1178 (4538)
	TY05		17607 $\pm$ 646 (1005)	17865 $\pm$ 665 (1035)	17172 $\pm$ 630 (1601)	17418 $\pm$ 648 (1648)
<b>Weighted mean</b>				<b>17430 <math>\pm</math> 700</b>		

and chisel (max sample depth 2 cm). As previous work has demonstrated that inheritance is rarely an issue in this region (Wilson et al., 2013a, 2013b; Livingstone et al., 2015), dual  $^{10}\text{Be}$  and  $^{26}\text{Al}$  isotope analysis was not conducted on the samples. All samples had their site context, position, altitude, topographic shielding, surface dip and dip direction, dimension, and all surface characteristics (e.g. pitted or spalled) recorded. Sites that could harbour snow, vegetation or sediment cover were avoided.

Samples were analysed in the Cosmogenic Isotope Analysis Facility (CIAF) at the Scottish Universities Environmental Research Centre (SUERC) according to standard protocols (Wilson et al., 2008).  $^{10}\text{Be}$  concentrations are based on  $2.79 \times 10^{-11}$   $^{10}\text{Be}/\text{Be}$  ratio for NIST S27900. The  $^{10}\text{Be}/\text{Be}$  ratios ranged between  $1.23 \times 10^{-13}$  and  $2.77 \times 10^{-13}$ . The processed blank ratio is detailed in Table 1, and was subtracted from the measured ratios. The uncertainty of this correction is included in the stated standard uncertainties.

Exposure ages and internal uncertainties (determined by the error in nuclide concentration) and external uncertainties (includes uncertainties in production rate) (Balco et al., 2008) were calculated using the CRONUS-Earth online calculators version 2.3 (<http://hess.ess.washington.edu/math/>; Wrapper script: 2.3; Main calculator: 2.1; Constants: 2.3; Muons: 1.1) (Balco et al., 2008). Results using the time-dependent Lal/Stone (Lm) scaling scheme are shown, and we use a reference SLHL production rate of  $4.00 \pm 0.17$  atoms  $\text{g}^{-1}$  quartz (cf. Fabel et al., 2012). This local production rate from Loch Lomond ensures compatibility with recently published BRITICE-CHRONO papers (Small and Fabel, 2015; Livingstone et al., 2015; Small et al., 2017). Results were calculated with a 0 and 0.0001 cm/yr erosion rate. However, at this scale, the differences in ages are within the uncertainties of the age, and so

the 0.0001 cm/yr erosion rate ages are applied. Ages from nearby sites (i.e. Wilson et al., 2013a; Livingstone et al., 2015) were recalculated according to these protocols to allow direct comparison.

We visualise cosmogenic nuclide ages on probability distributions (e.g., Kelly et al., 2008; Putnam et al., 2010; Balco, 2011; DeVecchio et al., 2012), where each age is represented with a Gaussian distribution, with mean and standard deviation corresponding to each individual measurement. This helps to describe the frequency distribution of the ages and identify outliers. Weighted mean ages of moraines ( $\mu_i \pm \sigma_i$ ) are calculated by excluding outliers and using the external uncertainties, to facilitate comparison to other published data.

#### 4. Geomorphology of the Eden Valley and Stainmore Gap

Geomorphological mapping revealed 1561 individual moraine mounds and ridges across the study area (Figs. 5 and 6). Also mapped are 677 new meltwater channels, 81 of which are related to ice-marginal positions. Together, these reveal a detailed and complex pattern of ice-marginal retreat in the Vale of Mowbray, across the Stainmore Gap and in the Vale of Eden (Fig. 5). Moraines and marginal meltwater channels clearly delineate multiple ice margins pertaining to a series of complex ice lobes. Analysis of these landforms, together with previously mapped bedforms (see Evans et al., 2017b, 2018; Clark et al., 2018) allows the identification of synchronous ice margins (Fig. 7).

The Vale of Mowbray is characterised by a series of moraines documenting, firstly, the lateral limits of the Vale of York Lobe (VY on Fig. 7), and the later separation of Wensleydale, Stainmore and North Sea Lobe ice (Figs. 5, 6b and 6c). This includes numerous

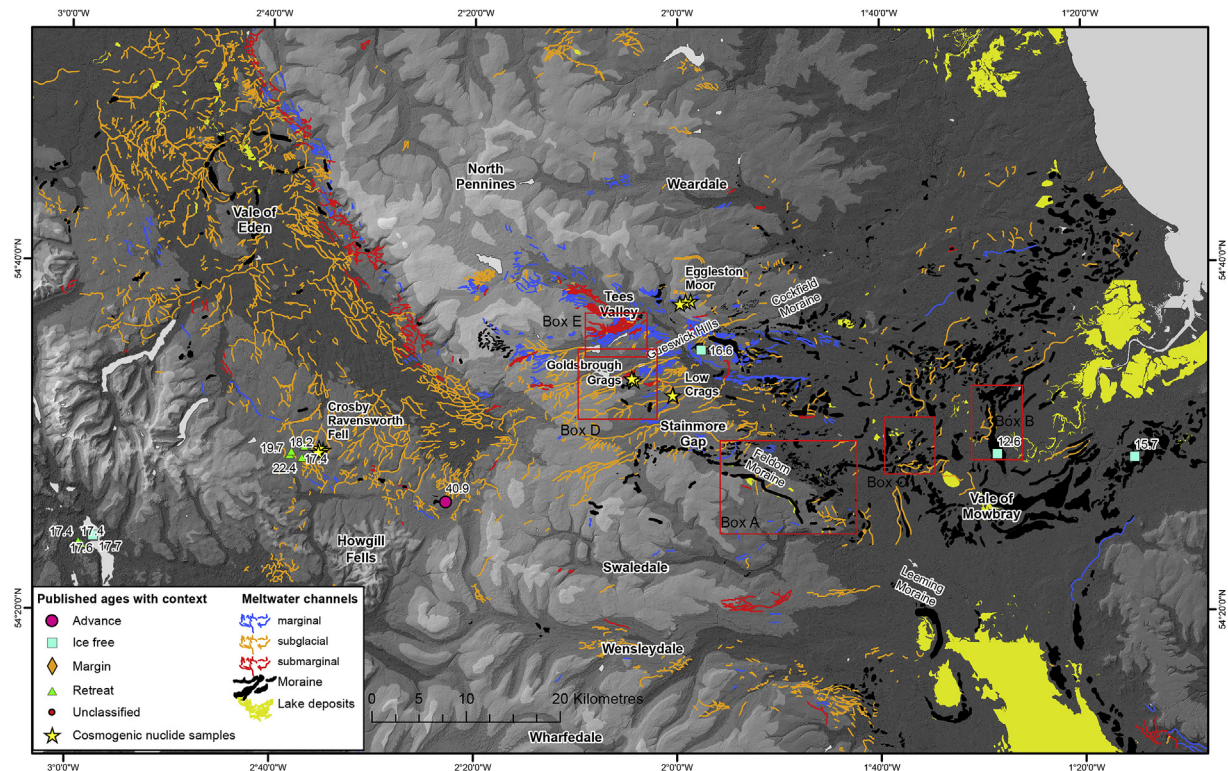


**Fig. 5.** New mapping and published geomorphology (Mitchell and Riley, 2006; Hughes et al., 2010; Bridgland et al., 2011; Evans et al., 2018) and the BRITICE V2 dataset (Clark et al., 2018). Meltwater channels mapped in this study and in BRITICE V2 are classified according to the criteria in Greenwood et al. (2007). Drumlins, meltwater channels and original mapped moraines are shown in Fig. 2 and 4. Note the new detail mapped in meltwater channel classification and in moraine extent in the Stainmore Gap and Vale of Mowbray. Boxes show location of examples A-E in Fig. 5.

small moraine mounds and ridges around the middle River Tees, in the western part of the Vale of Mowbray. Although fragmentary and dissected, they show two distinct families of nested, coherent lobate forms, one indicating ice flow from the east coast (VM on Fig. 7) and one out of the Stainmore Gap (ST). The VM family includes 5 distinct ice-marginal positions in the Vale of Mowbray, the oldest of which extends ~40 km into the lowlands from the present-day coast. The youngest inset moraine position (VM5) cross-cuts older moraines and is orientated more NW-SE along the present-day coastline.

At their western extent, the VM moraines are overprinted and cross-cut by moraines produced by Stainmore ice (Fig. 5b; ST on Fig. 7), indicating a >5 km re-advance of the Stainmore ice as a piedmont lobe into the Vale of Mowbray lowlands and over the older VM moraines. The Stainmore moraines indicate shifting ice flow patterns during recession. The oldest moraines (ST1-2) record ice flow southwards into the Vale of York. Later moraines (ST3-5) indicate a more easterly ice flow directly across Stainmore into the Vale of Mowbray. A younger Stainmore moraine (ST6), near Barnard Castle, indicates the influence of Teesdale ice flowing SE into the Stainmore Gap, while the central region comprises a series of discontinuous moraines of glaciotectonically displaced bedrock blocks (Fig. 5d; ST7; see Livingstone et al., 2017; Evans et al., 2018).

In the northern sector of the Stainmore Gap, just south of Middleton in Teesdale, there is a series of inset hummocky moraine mounds (Te on Fig. 7; Fig. 5e), which identify terminal positions of the ice margin. This documents the separation of Tees and Stainmore ice and recession of Tees ice back into upper Teesdale (see also Evans et al., 2018) (Fig. 5).

Like Stainmore, both Swaledale and Wensleydale contain a series of discontinuous moraine ridges and lateral meltwater

channels indicating lobate ice flow subsequent to the recession of the Vale of York Ice Lobe. Again, there is a shift from ice flowing out into the lowlands and turning to the south (W1), followed by more easterly flow as it recedes (W2-3 and S1).

Parallel and sub-parallel ice-marginal meltwater channels trending SE-NW along the flank of the North Pennines in the Vale of Eden clearly delimit a downwasting lateral ice margin (E1; Fig. 5) (cf. Greenwood et al., 2007; Livingstone et al., 2010c). There is a clear vertical limit, with marginal meltwater channels being limited to below 400 m (Fig. 5). We also map a series of arcuate cross-valley moraines demarcating three ice limits (E2-E3) in the Vale of Eden, and recording the final recession of Eden ice. The Penrith Sandstone outcrop, in the centre of the Vale of Eden, appears to have acted as a confining pinning point for the E3 and E4 ice margins (Fig. 5). At the northern end of the Vale of Eden, a receding ice margin is demarcated by the Brampton Kame Belt, which comprises a series of ridges, mounds, flat-topped hills and depressions (Trotter and Hollingworth, 1932; Huddart, 1981; Livingstone et al., 2010c; Lovell et al., 2019), and which forms the downstream expression of the subglacial and lateral meltwater channels along the lower slopes of the Pennine escarpment.

Eleven new cosmogenic nuclide samples were collected along a 60 km transect running west to east along the central trunk corridor of Stainmore Gap (Goldsborough and Low Crag), the main tributary glacier of Teesdale (Egglestone Moor) and the Vale of Eden at the onset of the Stainmore Ice Stream (Crosby Ravensworth Fell) (Table 1; Figs. 5–8). Sample ages are presented in Table 3 and graphically in Figs. 7 and 9. Although there is some scatter, there are sufficient samples to identify outliers (e.g. sample S10) by taking into account the spatial relationships between sample sites. Once outliers are excluded, uncertainty-weighted mean ages are



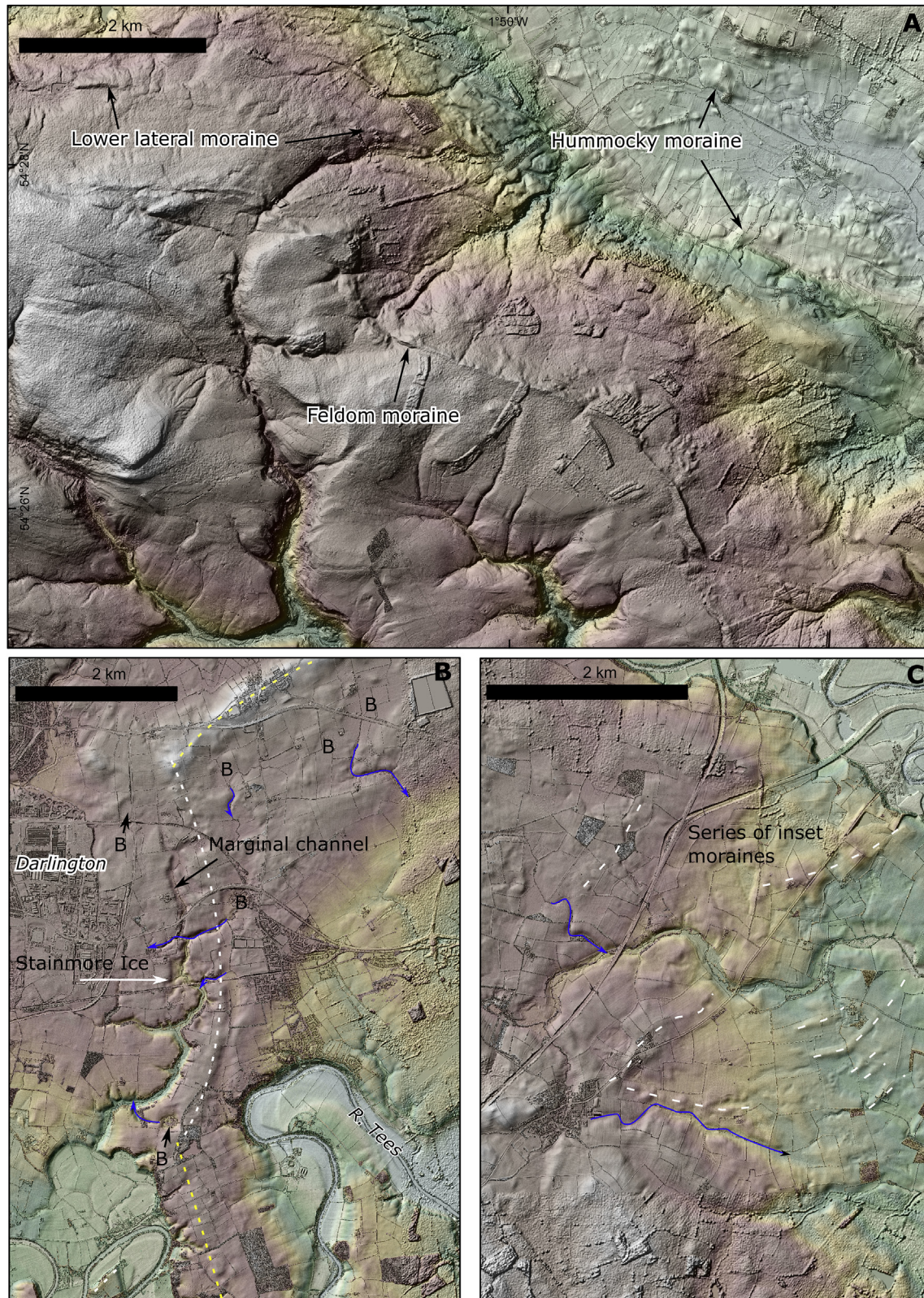


**Fig. 6.** Examples of morainic mounds and ridges. Locations of examples are shown in Fig. 5. A. Thinning of the southern lateral margin of the Stainmore Ice Stream delimited by the Feldom moraine (~380 m asl) and inset lateral moraines at lower elevations. B. Interplay between the North Sea Lobe (yellow dashed lines) and the Stainmore Lobe (white dashed lines), which has subsequently modified the moraine. B = basins and blue arrows = meltwater channels. C. SE margin of the Stainmore Ice Lobe in the Vale of Mowbray displaying series of inset moraine positions. D. Streamlined topography in Baldersdale, a western tributary to Teesdale. E. Lateral meltwater channels and streamlined topography at the confluence of lower Lunedale and upper Teesdale. (For interpretation of the references to colour in this figure legend, the reader is referred to the Web version of this article.)



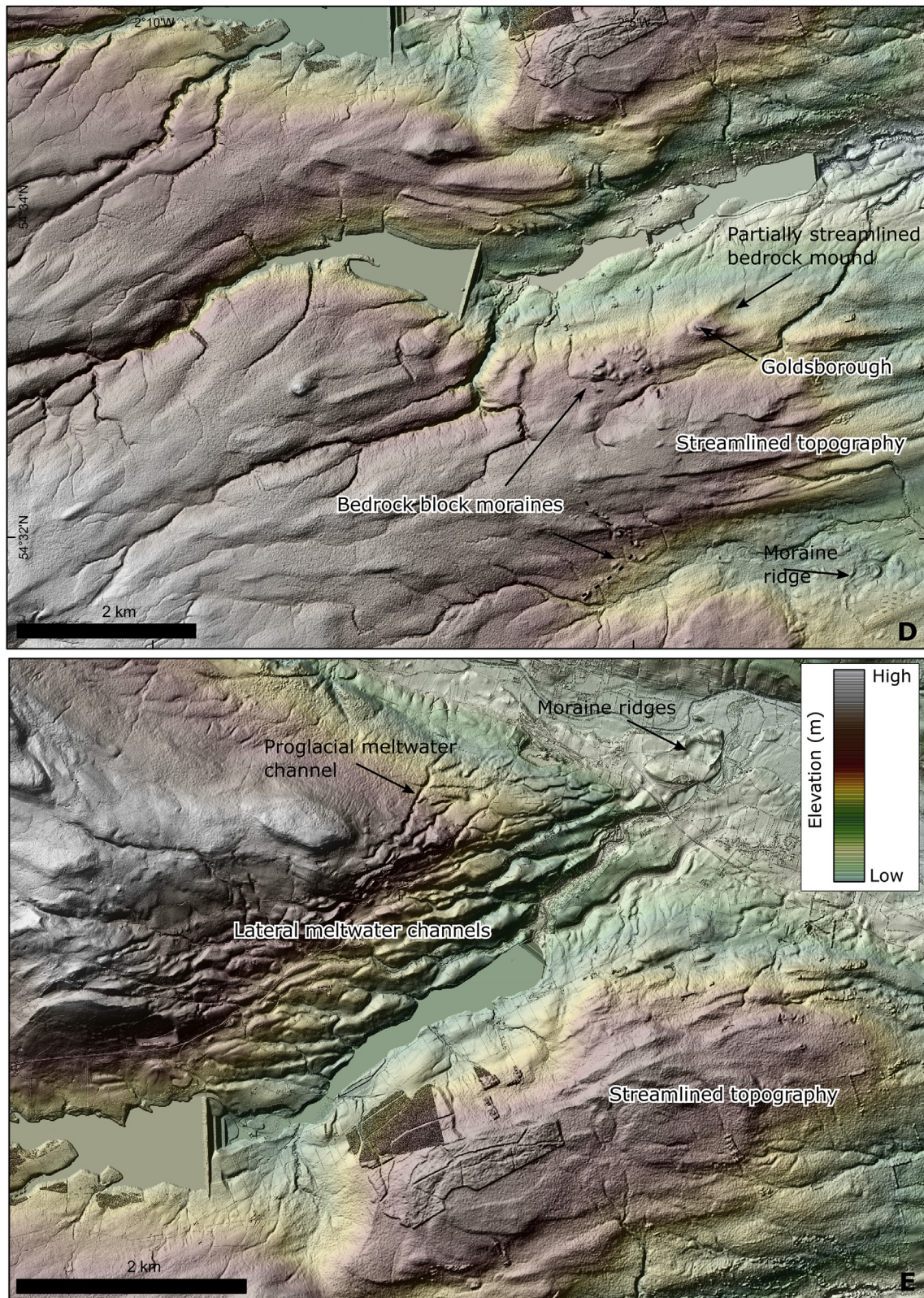


Fig. 6. (continued).

calculated for each sample site. In this section, we include recalculated ages from [Wilson et al. \(2013b\)](#) and [Livingstone et al. \(2015\)](#) for comparison.

Samples S02, S03 and S04 were taken from Shap granite erratics perched on the limestone plateau on Crosby Ravensworth Fell

(350–370 m asl), north of Orton, in eastern Cumbria ([Fig. 5](#); [Fig. 8](#)), near to the samples analysed in [Wilson et al. \(2013b\)](#) and 7 km from the Shap Granite outcrop. These samples are at the southern edge of flowset LT6 ([Fig. 4](#)) and therefore constrain the final southwards recession of ice from the Vale of Eden, and the separation of ice



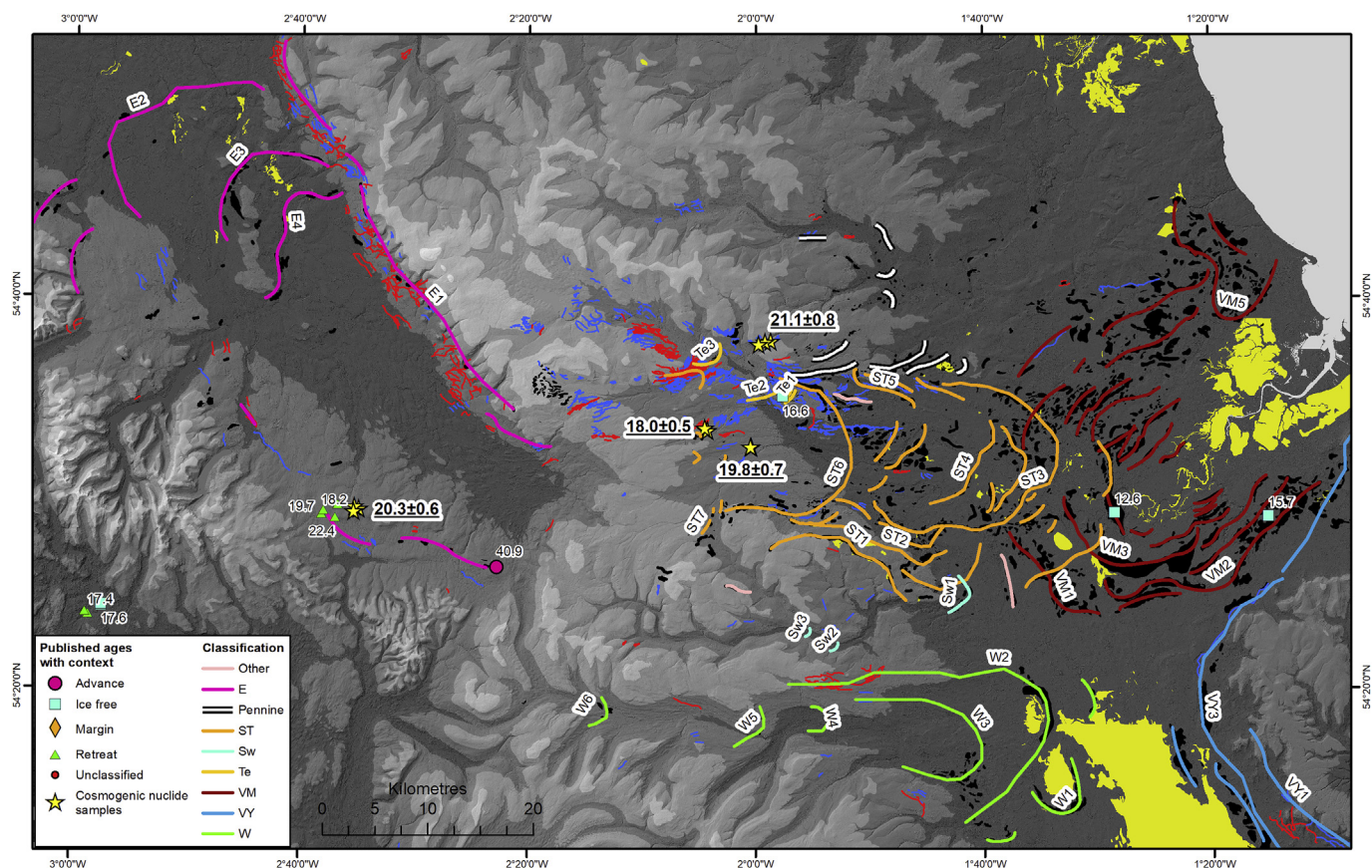


**Fig. 7.** Reconstruction of ice limits, showing the separation of the Stainmore (ST) and East coast ice in the Vale of Mowbray, and recession in the Vale of Eden. New cosmogenic nuclide ages are shown (underlined) with weighted means (see Table 2). New and published geomorphology constraining ice-marginal positions (e.g. newly classified meltwater channels and moraine ridges (Clark et al., 2018; Evans et al., 2018); and published ages are shown (Wilson et al., 2013a; Livingstone et al., 2015; Hughes et al., 2016). Classification of ice limits: E: Eden; ST: Stainmore; Sw: Swaledale; Te: Tees; VM: Vale of Mowbray; VY: Vale of York; W: Wensleydale. Geomorphological symbology as in Fig. 5. Marginal meltwater channels shown in blue, submarginal meltwater channels shown in red. Chronology of the Stainmore Gap Ice Stream. (For interpretation of the references to colour in this figure legend, the reader is referred to the Web version of this article.)

masses into the Lake District to the west and the Yorkshire Dales (cf. Wilson et al., 2013b). Although the samples show some scatter (between 17.4 and 23.9 ka), they yield a weighted mean age of  $20.3 \pm 0.6$  ka (Table 2). The nearby samples analysed in Wilson et al. (2013a) from Eastern Cumbria have a similar weighted mean age of  $19.2 \pm 0.6$  ka (Fig. 9).

Samples S05 and S06 were bedrock samples taken in the centre of the Stainmore Gap from Low Crag (310 m asl), a Carboniferous sandstone crag trending west-east. Low Crag is located in a region of rolling, glacially streamlined terrain within the main W-E orientated flowset (ST1–2, Fig. 4) of the Stainmore Gap Ice Stream (Fig. 5; Fig. 8). Both samples were taken from a slightly raised (~30 cm above grass) flat, partially abraded and jointed upper bedrock surface and have a weighted mean age of  $19.8 \pm 0.7$  (Table 2).

Goldsborough Crag (samples S07, S08 and S09) is a Carboniferous sandstone monadnock within the W-E glacially streamlined Stainmore Gap (Fig. 5; Fig. 8). Samples S07 and S08 were taken as a bedrock-erratic pair from the northern end of the monadnock (390 m asl), with S07 from a large Shap granite erratic boulder standing 1.8 m above ground level and Sample S08 from Carboniferous sandstone bedrock. Sample S09 was taken from a well-embedded Shap granite erratic boulder on a gentle slope (10°) just to the north of the crags. These samples lie some 41 km east of the Shap Granite outcrop, and delimit recession of ice flowing west to east across the Stainmore Gap. The three samples from Goldsborough Crag have a weighted mean age of  $18.0 \pm 0.5$  (Table 2).

Egglestone Moor is an undulating, rolling, upland surface in upper Teesdale. Three samples were taken (S10–S12) to constrain the recession of Teesdale ice to the upland Northern Pennines, and are the highest of all the new samples reported here (422 m, 416 m and 385 m asl respectively). Egglestone Moor comprises a thin drift cover over Carboniferous Sandstone and grit. S10 is a well-embedded sandstone boulder (Table 1) adjacent to a large shallow meltwater channel. Sample S11 is a bedrock sample of Carboniferous Sandstone that stands 1 m above local ground level at the onset of the meltwater channel. Finally, sample S12 is a well-embedded sandstone erratic boulder standing 0.4 m above local ground level. At Egglestone Moor, the highest sample, S10 is substantially older (35.4 ka) than all the other boulders sampled. Given the marginal, upland location of this sample we suggest it was incompletely reset, and is therefore excluded as an outlier. The weighted average age for this site, excluding S10, is  $21.1 \pm 0.8$  ka (Table 2).

The weighted mean of the central Tyne Gap samples from Livingstone et al. (2015; Fig. 1) is  $18.4 \pm 0.8$  ka, similar to Goldsborough and Low Crag from the central Stainmore Gap. Fig. 9H and I shows the variation of  $^{10}\text{Be}$  cosmogenic nuclide age with elevation and longitude (i.e. the transect along the Stainmore Gap). Ages from this study are compared with nearby published ages (Wilson et al., 2013a; Livingstone et al., 2015), which show consistency with altitude. There is an increase in sample age with altitude, which may be indicative of early thinning and the emergence of nunataks in the area, although it is also possible that the two highest samples



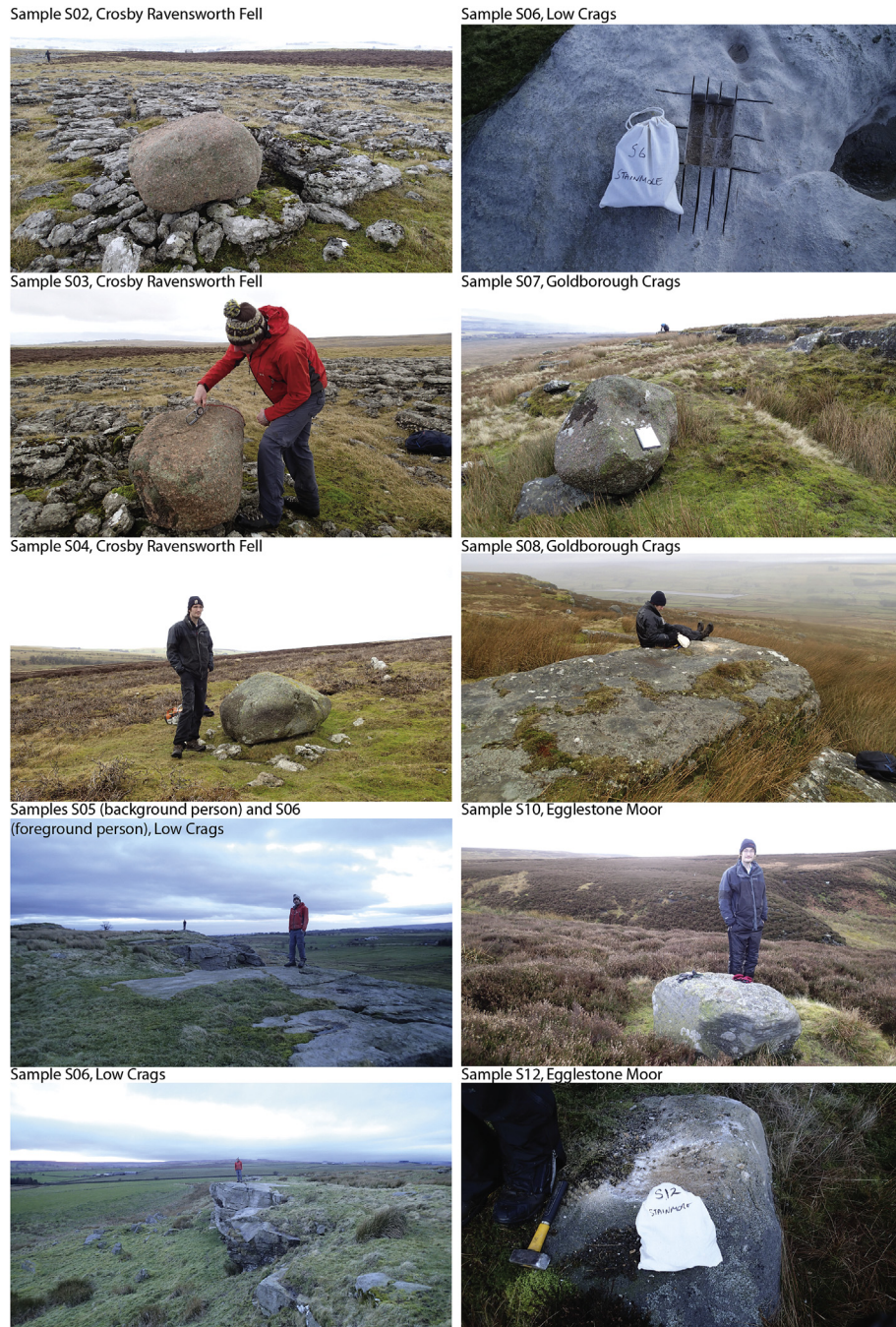


**Fig. 8.** Representative photographs of cosmogenic nuclide samples.

in Livingstone et al. (2015) and in this study have nuclide inheritance (potentially because thinner ice is less erosive). We have sampled carefully in this study to avoid issues with likely inheritance, and the closer clustering of our samples suggests that this is less of an issue in these samples.

## 5. Discussion

### 5.1. The nature and timing of the deglaciation of the Eden-Stainmore Ice Stream

Previous mapping of subglacial bedforms in the Eden-Stainmore region of the BIIS indicates two major flow periods: (1) initial

unconstrained west to east flow of the Eden-Stainmore Ice Stream from the Lake District and Scotland through the Stainmore Gap and into the Vale of York where it coalesced with the Vale of York Ice Lobe (LT1-2); and (2) shut down of the regionally driven Eden-Stainmore Ice Stream, due to a flow reversal in the Vale of Eden northwards into the Solway Lowlands, and subsequent SE flow of the topographically constrained Teesdale Glacier nourished by the North Pennines (Livingstone et al., 2008, 2012; Evans et al., 2018). Our new mapping and geochronological data help constrain the decoupling of the Stainmore and North Sea lobes in the Vale of Mowbray, the retreat of the Eden-Stainmore Ice Stream and the northwards switch in ice flow in the Vale of Eden.

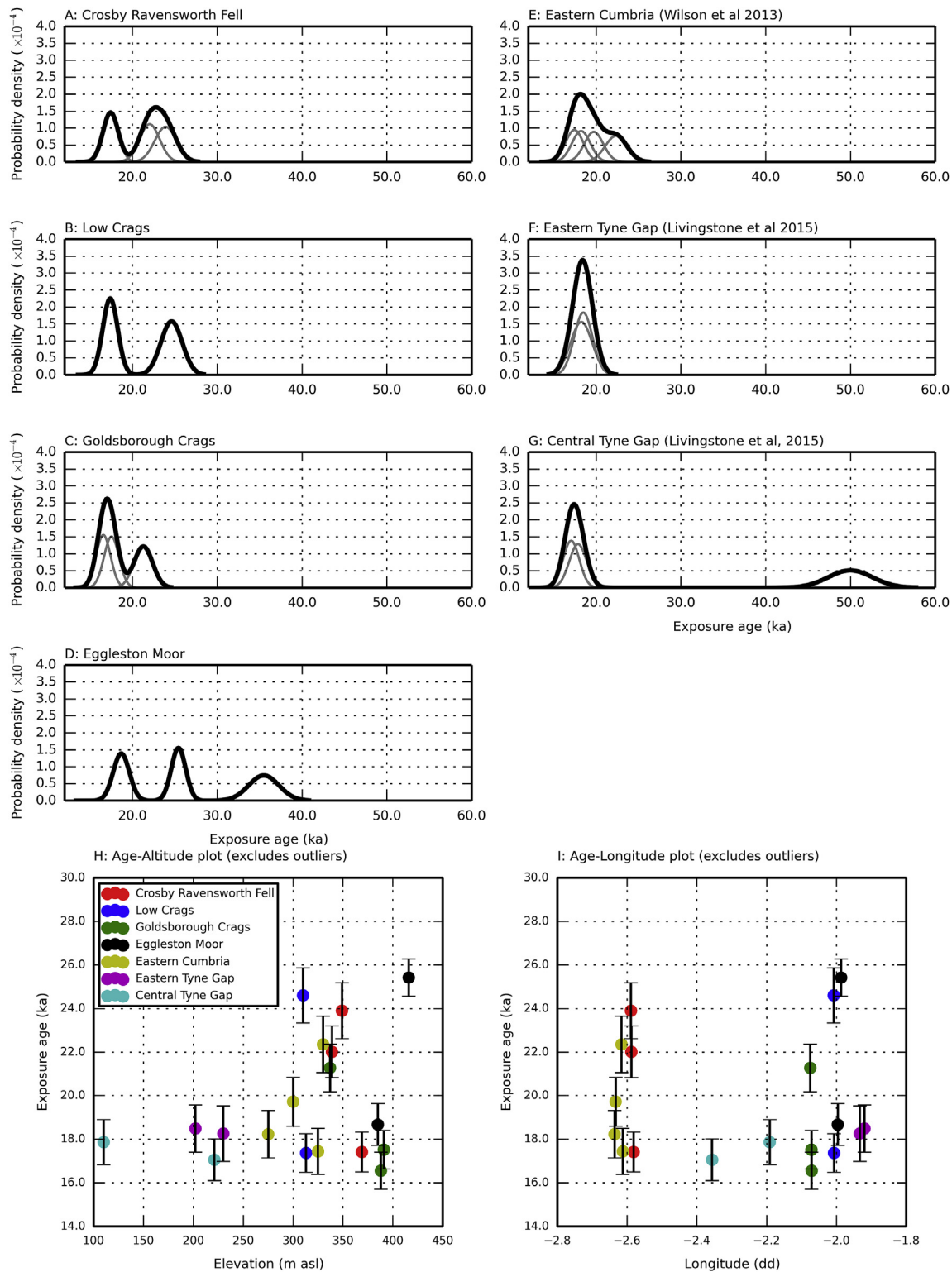


**Fig. 9.** “Camel plot” of the calculated cosmogenic nuclide ages at each site, using external uncertainties (0.0001 cm/yr erosion rate). Each Gaussian near the bottom of the plot represents a single age, with the width corresponding to  $1\sigma$  error in the age uncertainty (internal uncertainties), and each Gaussian has the same area. So high, narrow Gaussians have more precise age determinations. The smooth black line was created by summing the Gaussians. The peak age of a distribution highlights clusters of ages. Code to generate plots was created in Matplotlib, modified from [Balco \(2009\)](#).

### 5.1.1. Separation of the Stainmore and North Sea lobes in the Vale of Mowbray before 19 ka

Geomorphological data indicate that, at its maximum extent, the Vale of York Lobe may have reached the Lindholme Moraine at

Wroot, but it certainly occupied the York and Esrcick moraines in the southern Vale of York ([Figs. 1 and 4](#); [Bateman et al., 2015](#); [Friend et al., 2016](#)). Drumlins and clast lithological data indicate that the Vale of York Lobe was composed largely of ice from the Tees,



Wensleydale, Swaledale and Stainmore (Friend et al., 2016; Bateman et al., 2015, 2018; Evans et al., 2018; Clark et al., 2018). An initial advance of ice down the Vale of York may have occurred as early as 24.1–23.3 ka with sites at Kelsey and Hemingborough relating to lake impoundment and pre-dating till emplacement (Bateman et al., 2000). However, the main ice advance to the York – Escrick moraine complex (Fig. 4) (and possibly further south of this, to the Wroot limit) occurred at ~22 ka and is constrained by multiple OSL ages from lake and outwash sediments (Murton et al., 2009; Bateman et al., 2015; Friend et al., 2016). Based on these new geomorphological mapping and deglacial ages (Fig. 7, Table 3), ice then retreated over 60 km back up the Vale of York and westwards across Stainmore by 19.8 ka – 18.0 ka (i.e. within the error of the ages). This is compatible with a suite of deglacial ages from the Wroot limit (19.9–18.9 ka; Bateman et al., 2015) and further north at Ferrybridge (20.5 ka; Bateman et al., 2008).

In the Vale of Mowbray, extensive inset moraines document oscillatory retreat and competition between ice from both Eden-Stainmore and the North Sea as it separated into constituent flow lobes. Across the floor of the Tees basin, an upper till with Cheviot erratics (e.g. at Catterick and Scorton) indicates westward incursion of the North Sea Lobe almost to the eastern flanks of the northern Pennines (Mitchell et al., 2010), although there is also clear evidence that Eden-Stainmore ice later overprinted some of the more westerly North Sea Lobe moraines (VM1 on Fig. 7), thereby indicating ice margin oscillation during retreat. This early deglaciation of the lateral margin of the North Sea Lobe in the Vale of Mowbray may have coincided with ice retreat from North Norfolk and the Humber region in the North Sea from 21–19 ka (Roberts et al., 2018a, b) and preceded the damming of Glacial Lake Tees (Agar, 1954). Glaciers in major valleys emanating from the Pennine hills, such as Wensleydale and Swaledale, formed piedmont lobes in the Vale of York lowland as they ceased to be constrained by the southerly flowing Vale of York Lobe. Ice from Wensleydale spread laterally as it exited the confines of this narrow Pennine valley; the older W1 moraines show a more southerly orientation compared with the younger W2 recessional moraines (Leeming moraine; Bridgland et al., 2011) suggesting that they were initially deflected southwards by ice to the north (Fig. 7).

### 5.1.2. Ice recession through Stainmore Gap and uncoupling from upper Teesdale ice ~19 ka

The new cosmogenic nuclide ages in this study indicate that the Eden-Stainmore Ice Stream had receded to the central part of the Stainmore Gap by ca. 19 ka and that complete deglaciation of the Stainmore Gap occurred within the error range of these new ages, between ~20–18 ka (Fig. 9). This is supported by a radiocarbon age of  $16.6 \pm 0.5$  cal ka BP from Parrick House (Fig. 1; Innes and Evans, 2017), which provides a minimum age for ice retreat from the central Stainmore Gap. Samples from the Stainmore region are also within errors of those taken from the Tyne Gap, which became ice free in the eastern sector by  $18.4 \pm 0.8$  ka and in the central sector by  $17.4 \pm 0.7$  ka (Livingstone et al., 2015) (Table 3, Fig. 9). The pattern and rate of retreat for the Tyne and Eden-Stainmore palaeo-ice stream corridors was therefore broadly synchronous.

Moraines trending W-E along the southern flank of the Stainmore Gap, including the Feldom moraine (Figs. 5 and 6a; Kendall and Wroot, 1924), document progressive thinning of the lateral margin of the Eden-Stainmore Ice Stream from 380 to 330 m as it receded from the Vale of Mowbray (Bridgland et al., 2011). On the northern flank of the Tees Valley, deglaciation of Eggleston Moor suggests thinning and exposure of high terrain (>420 m) as early as  $21.1 \pm 0.8$  ka (Fig. 7), prior to or during ice-marginal recession from the Vale of Mowbray. As ice retreated back into the Stainmore area, inset moraines spanning the corridor record a change from

westwards (ST3–5) to north-westwards retreat (ST6) as northern Pennine ice became increasingly dominant and eastwards flowing Stainmore ice began to shut down. This was followed by localised and topographically constrained moraines and lateral meltwater channels documenting the uncoupling of Teesdale and Eden-Stainmore ice (ST7, Te 1–3).

Detailed geomorphological and sedimentological investigations in Teesdale reveal five inset assemblages of moraines and associated meltwater channels that record oscillations of the Teesdale and Stainmore ice during deglaciation (Evans et al., 2018). During the final Lonton stage, lateral meltwater channels demarcate the temporary development of cold-based or polythermal ice conditions around the margins of a plateau-based icefield (Fig. 6e), and have been correlated with locally derived glaciotectionised bedrock moraines in the middle and southern part of the Stainmore Gap (ST7; Fig. 6d), likely derived from quarrying under a frozen snout (Livingstone et al., 2017; Evans et al., 2018). Evans et al. (2018) assign this Lonton stage approximately to the Scottish Readvance. This agrees with the bounding ages, which suggest that retreat across Stainmore ~19 ka coincided with the Scottish Readvance into northern Cumbria at a similar time (Chiverrell et al., 2018), and that ice persisted in the Vale of Eden and Stainmore during this period (see below).

### 5.1.3. Ice flow reversal and recession through the Vale of Eden

The Vale of Eden deglaciated early, with the relatively high elevation Crossby-Ravensworth Fell samples (340–370 m asl) becoming exposed at  $19.1 \pm 0.6$  (Wilson et al., 2013a) to  $20.3 \pm 0.6$  ka (this study). That these ages are within error of the deglacial ages in the Stainmore Gap implies that both areas thinned near-synchronously. Thus a major flow reversal mapped in the Vale of Eden, flowing northwards into the Solway Lowlands and Irish Sea Basin (Rose and Letzer, 1977; Mitchell and Riley, 2006; Livingstone et al., 2008), must have occurred prior to ~20 ka. To explain this large-scale flow reversal, ice centres further north across southern Scotland must have thinned or shifted flow direction to allow ice dispersal centres across the Lake District, Howgill Fells, Yorkshire Dales and Alston Block to drive ice north-westwards down the Eden Valley. During this flow reversal, topography became more influential and important, suggesting thinner ice in general. At the northern end of the Vale of Eden, the Brampton Kame Belt formed during this phase of ice flow, forming a large area of glaciofluvial sediment (cf. Trotter and Hollingworth, 1932; Huddart, 1981; Livingstone et al., 2010c; Lovell et al., 2019).

This late stage and transient build-up of ice domes across high plateaus fringing the southern edge of the BIS towards the end of the LGM would have triggered the rapid regional shutdown of easterly flowing ice stream corridors as source areas and dispersal patterns shifted. Subsequent thinning and recession of the Vale of Eden ice is difficult to pin-point due to the lack of moraines or other ice-marginal evidence in this region. However, ice-marginal meltwater channels (Arthurton and Wadge, 1981; Greenwood et al., 2007; Livingstone et al., 2010) and a series of moraines (Fig. 5) indicate temporary stabilization against the Penrith sandstone outcrop document recession of ice in the Vale of Eden. The final phase of ice-flow northwards through the Vale of Eden must have been sourced from the Howgills and the Lake District, given the elevation of the meltwater channels. The Pennines were likely a small plateau ice field by this time.

Chiverrell et al. (2018) constrain the timing of the Scottish Readvance, which was thought to be a regional event across the Isle of Man and Cumbrian Lowlands, to 19.2–18.2 ka. This corresponds with the timing of rapid retreat back across the Tyne, Stainmore and Vale of Eden corridors, and implies asynchronous behaviour of Scottish and northern England ice dispersal centres during this



period. This hypothesis requires further testing, and a more robust chronology for the central sector of the BIIS is needed to fully disentangle regional ice dynamics. By 17 ka ice had retreated back into upland ice dispersal centres, such as the Lake District, and these were undergoing widespread thinning (e.g. [McCarroll et al., 2010](#); [Wilson et al., 2013b](#); [Wilson and Lord, 2014](#)).

## 5.2. Reconstruction of the central sector of the last British-Irish Ice Sheet

The new geomorphological mapping and age constraints reported here allow the reconstruction of a 4-stage model for ice retreat in the central sector of the BIIS ([Fig. 10](#)), which builds on recent models put forward by [Livingstone et al. \(2012, 2015\)](#) and [Roberts et al. \(2018a; b\)](#).

### 5.2.1. Stage I (LGM)

The Eden-Stainmore Ice Stream, with multiple source regions in the Southern Uplands, Lake District and Pennines, flowed through the Eden Valley and across the broad Stainmore Gap where it became confluent with the North Sea Lobe ([Fig. 10](#)). During the

early stages of the LLGM the Eden-Stainmore Ice Stream may have reached the east coast via the Tees basin as indicated by the Shap erratics train.

During the latter stages of the LGM (~22–20 ka) the rapid build-up of local ice masses across the Lake District, Northern Pennines and Yorkshire Dales triggered ice divide migration and flow reversal to the northwest along the Eden-Stainmore Ice Stream corridor.

The subsequent reduction in easterly ice flux may have facilitated the incursion of North Sea Lobe ice westwards through the Tees basin and into the Vale of Mowbray/York where a composite ice lobe formed. Coincident with, or shortly after this, a regional re-advance of the North Sea Lobe at ~22–21 ka in the North Sea ([Roberts et al., 2018a](#)) may have been responsible for the formation of the Esrick-York moraine complex, or for the moraine complex in the Vale of Mowbray. Clast lithological data from the Esrick-York moraine complex includes Carboniferous Limestone and sandstone, with sporadic volcanic material ([Murton, 2018](#)), suggesting that the Eden-Stainmore Ice Stream dominated ice flow into the Vale of York. However, clast lithological data from Lindholme, just south of the Esrick-York moraine complex ([Fig. 4](#)), includes

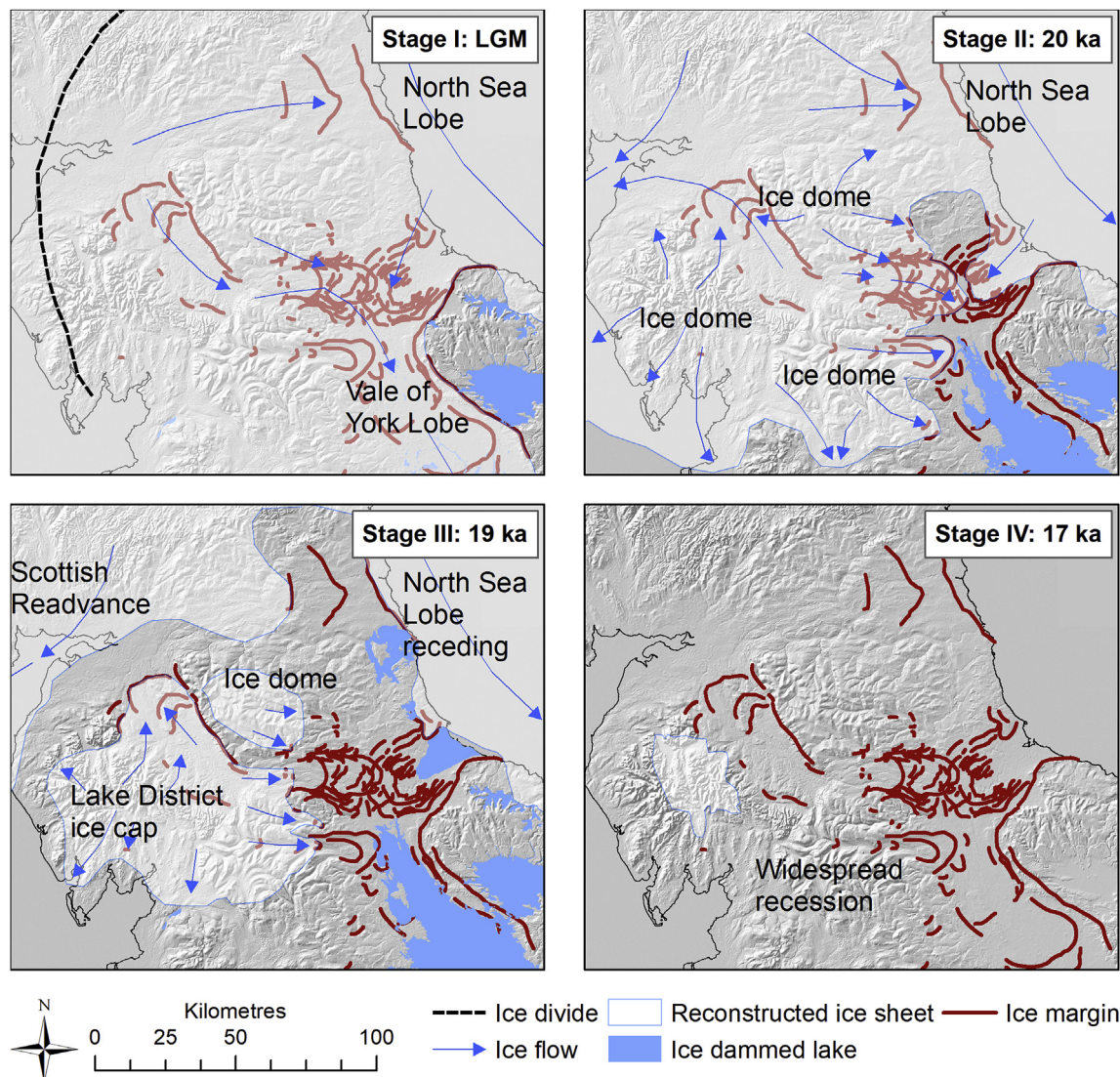


**Fig. 10.** Palaeo ice-sheet reconstruction of the central sector of the last British-Irish Ice Sheet.

Permian Lower Magnesian Limestone from the east coast of northern England (Bateman et al., 2015), suggesting some input from the North Sea Lobe and supporting a composite ice lobe.

### 5.2.2. Stage II (20 ka)

The North Sea Lobe and Eden-Stainmore Ice Stream deglaciated at approximately the same time, although in the Vale of Mowbray recessional moraines from the Eden-Stainmore Ice Stream overprint North Sea Lobe moraines, suggesting minor asynchronicity between the two ice masses in the window 21–19 ka (Figs. 6 and 7).

The growing dominance of local ice domes over the Lake District, central Pennines and Yorkshire Dales towards the end of the LGM caused major regional-scale changes to ice flow configuration. Our new ages from Egglestone Moor at 385–416 m asl support thinning and increasing topographic focusing in the Stainmore Valley at  $21.1 \pm 0.8$  ka. The Feldom moraine along the southern flank of the Stainmore Gap (Fig. 5a; Fig. 5; Kendall and Wroot, 1924) also documents progressive thinning of the lateral margin of the Eden-Stainmore Ice Stream from 380 to 330 m as it receded from the Vale of Mowbray.

### 5.2.3. Stage III (19 ka)

Following the flow reversal in the Eden Valley, the Stainmore-Eden corridor deglaciated between 19.8 and 18.0 ka (Fig. 10) with the central Tyne Gap also deglaciating around this time (18.5–17.1 ka). The Brampton Kame Belt formed in the Solway Lowlands as the Vale of Eden ice lobe and Tyne Gap ice lobe receded. Ice in the Vale of Eden receded rapidly, forming cross-valley moraines, in line with the broader regional deglaciation, and ice in the Lake District was confined to valley glaciers. Hence, while the Tyne Gap and Eden-Stainmore ice stream corridors were downwasting, the Scottish Re-advance was underway, suggesting that the Southern Upland ice dispersal centres were once again being nourished (Stage III; Chiverrell et al., 2018). McCabe et al. (1998) relate this to Heinrich I and North Atlantic cooling, although Chiverrell et al. (2018) have recently highlighted the challenges of cross-correlating multiple regional re-advances with discrete climate events.

The North Sea Lobe remained along the coast of County Durham until ~19 ka, (damming Glacial Lake Wear; Roberts et al., 2018b), but ice had left the Yorkshire coast by this time. Hence glacial lakes Humber, Pickering and Tees may have only been partially dammed by moraines by this time.

### 5.2.4. Stage IV (17 ka)

By 17 to 16.5 ka, the North Sea Lobe had receded completely from the east coast of England and reached the Firth of Forth (Roberts et al., 2018b). The final stages of glaciation inland saw the establishment of a plateau ice field over the Pennines and a local ice cap over the Lake District (Fig. 10; Stage IV). This plateau ice field was likely deglaciated before 17 ka, but the Lake District ice cap endured for longer, due to the higher elevation of the terrain. The central Stainmore corridor was ice-free. The radiocarbon age ( $16.6 \pm 0.5$  cal ka BP) from Parrick House (Fig. 1; Innes and Evans, 2017) is consistent with the cosmogenic nuclide ages from the nearby Goldsborough Crags and Low Crags in the central Stainmore Gap.

## 5.3. Implications for ice dynamics

This study highlights the presence of dynamic and land-terminating ice streams in the central sector of the last BIIS from the LLGM through to deglaciation; most work to date has focused on ice streams that terminated offshore, on the continental shelf, at the margins of the BIIS (e.g. Stoker and Bradwell, 2005; Livingstone et al., 2012; Krabbendam et al., 2016; Chiverrell et al., 2018; Roberts

et al., 2018a). The land-terminating Vale of York ice stream terminated in a shallow lake, a rare example within the last BIIS. Glacial Lake Humber was rather shallow, with the presence of moraines suggesting an ice margin with limited calving. As a land-terminating ice stream is more isolated from marine controls on ice dynamics (i.e. sea surface temperatures, bathymetry and water depth, ocean currents), the Vale of York Lobe may have been responding to different external controls to those driving ice stream dynamics around the rest of the BIIS, although we note that the North Sea Lobe was also terrestrial during its early recession.

The Eden-Stainmore and North Sea Lobe ice streams were highly dynamic, with major flow shifts and flow reversals over the short timeframe of 1000 years. Our new data provide insights into the timing of major reorganisations close to the centre of the last BIIS, with a highly unusual major change in palaeo ice-flow direction of close to  $180^\circ$  driven by changing regional ice divides, and with ice flow being increasingly controlled topographically as the ice sheet thinned during early deglaciation. This thinning was likely driven by external factors related to changes in the oceanic and climatic system. Deglacial changes in ice stream flow are not unusual in palaeo-ice sheets, but flow reversals similar to those of the Eden-Solway system are less common. For example, less substantial changes in palaeo ice-flow direction have been observed in the Antarctic Peninsula, with palaeo ice flow being increasingly driven by thinning during deglaciation (e.g., Glasser et al., 2014). In Ireland, flowset cross-cutting is prevalent, indicating major ice-divide migrations and changes in the flow configuration of the ice sheet (Greenwood and Clark, 2009). Here, late-stage flowsets again reflect increasing control by local topographic factors. In North America, palaeo ice-streams showed dynamic behaviour over low-relief areas, with a 'switching' behaviour driven by changes in geology and topography during recession, competition between neighbouring catchments (in terms of ice and subglacial melt-water), and surging behaviour, as well as potential external climate triggers (Dyke and Prest, 1987; Ó Cofaigh et al., 2010; Evans et al., 2008, 2014; Margold et al., 2015).

These topographically driven ice streams contrast with the rapid change in marine-terminating ice-stream organisation currently seen in Antarctica, for example, with Kamb and Institute ice streams on the Siple Coast (e.g. Catania et al., 2006; Conway et al., 2002; Joughin et al., 2005; Siegert et al., 2013). Ice flow direction change of  $\sim 45^\circ$  is also recorded in fold structures in ice layers in the interior of West Antarctica (Siegert et al., 2004). This fold axis is more than 50 km long, aligned at up to  $45^\circ$  to present-day ice flow direction. This modern analogue provides a mechanism by which ice flow direction can evolve over time. These rapid changes in the Antarctic Siple Coast are highlighted by relict longitudinal surface structures such as flow stripes, which are no longer aligned with the direction of ice flow (Ely and Clark, 2016; Ely et al., 2017). These marine-terminating ice streams all drain in predominantly the same direction, and compete for ice among their own catchments. In these cases, ice stream shutdown may be driven by internal controls (e.g. water piracy, bed stiffening; cf. Anandakrishnan and Alley, 1997; Alley et al., 1994; Carter et al., 2013), in contrast to our study region.

In contrast, palaeo ice sheets and ice fields that are nourished by Alpine topography (e.g. European Alps, New Zealand, Patagonia, North American Cordillera), tend to remain topographically controlled throughout full glaciation, and so do not record similar evidence of changes in palaeo ice-flow direction during deglaciation (e.g. Barrell, 2011; Coronato and Rabassa, 2011; Glasser et al., 2008).

There is a growing body of work that suggests that these large-scale reorganisations of ice flow are a common and normal response of ice sheets to rapid external and internal forcing. This



could be expected to occur as a result of changing ice divides and shifting centres of accumulation in a rapidly changing ice mass in a variety of different circumstances and environments (Clark, 1997; Kleman et al., 2006), but topographic forcing of ice flow must become increasingly important in the later stages of glaciation where thinning exposes closely spaced upland massifs, as in the central sector of the last BIIS. It is likely that the very significant changes in palaeo-ice flow direction observed in the Vale of Eden was a rare consequence of the local and regional topography and geology, with a multitude of regional ice dispersal centres, upon which complex ice-divide migration took place during ice-sheet thinning. This work highlights the potential for major ice-flow reorganisations close to the centre of a large ice sheet, and the importance of variation in local upland centres of ice dispersion for driving ice flow.

#### 5.4. Key unknowns in the post-LGM evolution of the central sector of the BIIS

This work, and on-going research in the area, highlights a number of remaining key research questions. Firstly, chronological control for ice recession from the Lake District, Howgill Fells and key valleys in the Yorkshire Dales remains elusive. The recession of the southern margin of the ice sheet throughout the Late Glacial remains poorly constrained. In our new model, ice extent in this region after 19 ka remains highly speculative. The presence of plateau icefields in the North Pennines during the Late Glacial has been established from geomorphological mapping in Teesdale (Evans et al., 2018), but is not yet established south of the Stainmore Gap; detailed geomorphological mapping and landsystems analysis is required in these valleys. The presence of ice in these Pennine uplands during the Younger Dryas glaciation is also unresolved (cf. Manley, 1961; Wilson and Clark, 1995; Mitchell, 1996; Evans and Jamieson, 2017). Further chronological control would help to understand links to wider atmospheric circulation and broader climatic controls, and would enable a higher degree of confidence in assessing the (a) synchronicity of recession in different parts of the ice margin. These kinds of data are required in order to fully assess ice-sheet response to rapid external climatic forcing, which is critical if we are to combine geomorphological, geochronological and palaeoclimatic data in numerical ice-sheet models (cf. Evans et al., 2009; Hubbard et al., 2009; Ely et al., 2019), and use these data to improve our understanding of present-day ice-sheet change.

## 6. Conclusions

This study aimed to determine the nature and timing of deglaciation in the central sector of the last BIIS, specifically in the Vale of York, Vale of Mowbray, Eden Valley and Stainmore valley. The new geomorphological mapping of moraines and meltwater channels, together with 11 new  $^{10}\text{Be}$  surface exposure ages on glacially transported boulders and glacially eroded bedrock, allow us to constrain ice-stream retreat following the LGM in northern England. These new data reveal 1561 individual moraines and 677 new meltwater channels that can be related to 108 ice-marginal positions.

The new data reveal a complex pattern of ice-stream recession and separation in the Vale of Mowbray, across the Stainmore Gap and in the Vale of Eden. Extensive inset moraines here document oscillatory retreat and competition between the Eden-Stainmore Ice Stream, which sourced the Vale of York Ice Lobe, and North Sea Lobe, as the ice separated into constituent flow units. These new data are used to produce a 4-stage model for ice retreat in the central sector of the BIIS (Fig. 10).

During the early stages of the LGM, the Eden-Stainmore Ice Stream reached the east coast via the Tees Basin. By ~20 ka, this easterly ice flow was reduced and the ice stream began to wane. This facilitated westwards incursion of the North Sea Lobe into the Tees basin and possibly down the Vale of York, and may have coincided with a regional re-advance of the North Sea Lobe at ~22–21 ka in the North Sea. Dynamic interactions between the two ice lobes are recorded in the multitude of ice margins recorded in the Vale of Mowbray. At ~21–19 ka, valley glaciers emanating from the Pennine Hills (such as Wensleydale and Swaledale) formed piedmont lobes in the Vale of York lowlands, as they ceased to be constrained by ice in the central valley.

The Stainmore corridor became ice free by 19.8 ka – 18.0 ka, coincident with the recession of the Tyne Gap Ice Stream further to the north. As the Stainmore Ice Stream waned, northern Pennine ice became increasingly dominant. Localised and topographically constrained moraines and lateral meltwater channels document the separation of Teesdale and Eden-Stainmore ice. By 17 ka, ice had retreated back into upland ice-dispersal centres. These data highlight the importance of complex topography and regional competing ice dispersal centres in driving ice sheet dynamics, ice divide migration and ice flow during regional thinning, and how these internal controls can modulate and influence a broader response to external climate and oceanographic controls on ice sheet dynamics.

## Acknowledgements

Cosmogenic nuclide ages were funded by NERC CIAF grant 9149.1014. The authors acknowledge the Quaternary Research Association (QRA) for a QRA Research Award which helped finance fieldwork. The authors acknowledge the landowners for generous access to their land. The authors thank Jenny Thornton for cartographic and GIS assistance. The authors thank Mark Bateman for a number of constructive comments on the new reconstruction. We thank two anonymous reviewers for comments that improved the manuscript. Supporting data is included in the manuscript and can also be obtained by emailing the authors on [rdm@royalholloway.ac.uk](mailto:rdm@royalholloway.ac.uk).

## Appendix A. Supplementary data

Supplementary data to this article can be found online at <https://doi.org/10.1016/j.quascirev.2019.105989>.

## References

- Agar, R., 1954. Glacial and post-glacial geology of Middlesbrough and the Tees estuary. *Proc. Yorksh. Geol. Soc.* 29, 237–253.
- Aitkenhead, N., Barclay, W.J., Brandon, A., Chadwick, R.A., Chisholm, J.L., Cooper, A.H., Johnson, E.W., 2002. *British Regional Geology: the Pennines and Adjacent Areas*, fourth ed. British Geological Survey, Nottingham.
- Alley, R.B., Anandakrishnan, S., Bentley, C.R., Lord, N., 1994. A water-piracy hypothesis for the stagnation of Ice Stream C, Antarctica. *Ann. Glaciol.* 20, 187–194.
- Anandakrishnan, S., Alley, R.B., 1997. Stagnation of ice stream C, West Antarctica by water piracy. *Geophys. Res. Lett.* 24, 265–268.
- Arthurton, R.S., Wadge, A.J., 1981. *Geology of the Country Around Penrith*. HMSO, London.
- Balco, G., 2009. MATLAB Code for Camel Diagrams. <https://cosmognosis.wordpress.com/2009/07/13/matlab-code-for-camel-diagrams/>.
- Balco, G., 2011. Contributions and unrealized potential contributions of cosmogenic-nuclide exposure dating to glacier chronology, 1990 – 2010. *Quat. Sci. Rev.* 30, 3–27.
- Balco, G., Stone, J.O., Lifton, N.A., Dunai, T.J., 2008. A complete and easily accessible means of calculating surface exposure ages or erosion rates from  $^{10}\text{Be}$  and  $^{26}\text{Al}$  measurements. *Quat. Geochronol.* 3, 174–195.
- Bamber, J.L., Vaughan, D.G., Joughin, I., 2000. Widespread complex flow in the interior of the Antarctic ice sheet. *Science* 287, 1248–1250.
- Barrell, D.J.A., 2011. Chapter 75 – Quaternary glaciers of New Zealand. In: Jürgen



- Ehlers, P.L.G., Philip, D.H. (Eds.), *Developments in Quaternary Sciences*. Elsevier, pp. 1047–1064.
- Bateman, M.D., Evans, D.J., Roberts, D.H., Medialdea, A., Ely, J., Clark, C.D., 2018. The timing and consequences of the blockage of the Humber Gap by the last British–Irish Ice Sheet. *Boreas* 47, 41–61.
- Bateman D., M., Buckland C., P., Chase, B., Frederik D., C., Gaunt D., G., 2008. The Late-Devensian proglacial Lake Humber: new evidence from littoral deposits at Ferrybridge, Yorkshire, England. *Boreas* 37, 195–210.
- Bateman, M.D., Evans, D.J.A., Buckland, P.C., Connell, E.R., Friend, R.J., Hartmann, D., Neasham, H., Fairburn, W.A., Panagiotakopulu, E., Ashurst, R.A., 2015. Last glacial dynamics of the Vale of York and North Sea lobes of the British and Irish ice sheet. *Proc. Geologists' Assoc.* 126, 712–730.
- Bateman D., M., Murton B., J., Crowe, W., 2000. Late Devensian and Holocene depositional environments associated with the coversands around Caistor, north Lincolnshire. *Boreas* 16, 1–16.
- Bennett, M.R., 2003. Ice streams as the arteries of an ice sheet: their mechanics, stability and significance. *Earth Sci. Rev.* 61, 309–339.
- Blackburn, K., 1952. The dating of a deposit containing an elk skeleton found at Neasham, near Darlington, County Durham. *New Phytol.* 51, 364–377.
- Boston, C.M., Evans, D.J.A., Ó Cofaigh, C., 2010. Styles of till deposition at the margin of the Last Glacial Maximum North Sea Lobe of the British–Irish Ice Sheet: an assessment based on geochemical properties of glacial deposits in eastern England. *Quat. Sci. Rev.* 29, 3184–3211.
- Boulton, G.S., Smith, G.D., Jones, A.S., Newsome, J., 1985. Glacial geology and glaciology of the last mid-latitude ice sheets. *J. Geol. Soc. Lond.* 142, 447–474.
- Bridgland, D.R., Innes, J.B., Long, A.J., Mitchell, W.A., 2011. *Late Quaternary Landscape Evolution of the Swale-Ure Washlands*, North Yorkshire. Oxbow Books, Oxford.
- Carter, S.P., Fricker, H.A., Siegfried, M.R., 2013. Evidence of rapid subglacial water piracy under whillans ice stream, west Antarctica. *J. Glaciol.* 59, 1147–1162.
- Catania, G.A., Scambos, T.A., Conway, H., Raymond, C.F., 2006. Sequential stagnation of Kamb ice stream, west Antarctica. *Geophys. Res. Lett.* 33.
- Catt, J.A., 1991. The Quaternary history and glacial deposits of East Yorkshire. In: Ehlers, J., Gibbard, P., Rose, J. (Eds.), *Glacial Deposits in Great Britain and Ireland*. A. A. Balkema, Rotterdam, pp. 185–191.
- Chiverrell, R., Smedley, R., Small, D., Ballantyne, C., Burke, M., Callard, S., Clark, C., Duller, G., Evans, D., Fabel, D., 2018. Ice margin oscillations during deglaciation of the northern Irish Sea Basin. *J. Quat. Sci.* 33 (7), 739–762.
- Clapperton, C.M., 1970. The Evidence for a Cheviot Ice Cap. *Transactions of the Institute of British Geographers*, pp. 115–127.
- Clark, C.D., 1997. Reconstructing the evolutionary dynamics of former ice sheets using multi-temporal evidence, remote sensing and GIS. *Quat. Sci. Rev.* 16, 1067–1092.
- Clark, C.D., Ely, J.C., Greenwood, S.L., Hughes, A.L.C., Meehan, R., Barr, I.D., Bateman, M.D., Bradwell, T., Doole, J., Evans, D.J.A., Jordan, C.J., Monteys, X., Pellicer, X.M., Sheehy, M., 2018. BRITICE Glacial Map, version 2: a map and GIS database of glacial landforms of the last British–Irish Ice Sheet. *Boreas* 47, 11–e18.
- Clark, C.D., Evans, D.J.A., Khatwa, A., Bradwell, T., Jordan, C.J., Marsh, S.H., Mitchell, W.A., Bateman, M.D., 2004. Map and GIS database of glacial landforms and features related to the last British Ice Sheet. *Boreas* 33, 359–375.
- Clark, C.D., Hughes, A.L.C., Greenwood, S.L., Jordan, C., Sejrup, H.P., 2012. Pattern and timing of retreat of the last British–Irish Ice Sheet. *Quat. Sci. Rev.* 44, 112–146.
- Cockburn, H.A.P., Summerfield, M.A., 2004. Geomorphological applications of cosmogenic isotope analysis. *Prog. Phys. Geogr.* 28, 1–42.
- Conway, H., Catania, G., Raymond, C.F., Gades, A.M., Scambos, T., Englehardt, H., 2002. Switch of flow direction in an Antarctic ice stream. *Nature* 419, 465–467.
- Cooper, A.H., Burgess, I.C., 1993. *Geology of the Country Around Harrogate: Memoir for 1:50 000 Geological Sheet 62 (England and Wales)*. HMSO, London.
- Corbett, L.B., Young, N.E., Bierman, P.R., Briner, J.P., Neumann, T.A., Rood, D.H., Graly, J.A., 2011. Paired bedrock and boulder  $^{10}\text{Be}$  concentrations resulting from early Holocene ice retreat near Jakobshavn Isfjord, western Greenland. *Quat. Sci. Rev.* 30, 1739–1749.
- Coronato, A., Rabassa, J., 2011. Chapter 51 - pleistocene Glaciations in Southern Patagonia and Tierra del Fuego. In: Jürgen Ehlers, P.L.G., Philip, D.H. (Eds.), *Developments in Quaternary Sciences*. Elsevier, pp. 715–727.
- Dalton, A.C., 1941. Lake Humber as interpreted by the glaciation of England and Wales. *North West. Nat.* 16, 256–265.
- Darvill, C.M., 2013. Cosmogenic nuclide analysis. In: Clarke, L., Nield, J. (Eds.), *Geomorphological Techniques*. British Society for Geomorphology, London.
- Davies, B.J., Roberts, D.H., Bridgland, D.R., Ó Cofaigh, C., 2012. Dynamic Devensian ice flow in NE England: a sedimentological reconstruction. *Boreas* 41, 337–366.
- Davies, B.J., Roberts, D.H., Bridgland, D.R., Ó Cofaigh, C., Riding, J.B., 2011. Provenance and depositional environments of Quaternary sedimentary formations of the western North Sea Basin. *J. Quat. Sci.* 26, 59–75.
- Davies, B.J., Roberts, D.H., Bridgland, D.R., Ó Cofaigh, C., Riding, J.B., Phillips, E.R., Teasdale, D.A., 2009. Interlobate ice sheet dynamics during the last glacial maximum at Whitburn Bay, County Durham, England. *Boreas* 38, 555–575.
- Davies, B.J., Yorke, L., Bridgland, D.R., Roberts, D.H., 2013. *The Quaternary of Northumberland, Durham and North Yorkshire: Field Guide*. Quaternary Research Association, London.
- DeVecchio, D.E., Heermance, R.V., Fuchs, M., Owen, L.A., 2012. Climate-controlled landscape evolution in the western transverse ranges, California: insights from quaternary geochronology of the Saugus formation and strath terrace flights. *Lithosphere* 4, 110–130.
- Dyke, A., Prest, V., 1987. Late wisconsinan and Holocene history of the Laurentide ice sheet. *Géogr. Phys. Quaternaire* 41, 237–263.
- Edwards, W., 1937. A Pleistocene strand line in the Vale of York. *Proc. Yorks. Geol. Soc.* 23, 103–118.
- Ely, J.C., Clark, C.D., 2016. Flow-stripes and foliations of the Antarctic ice sheet. *J. Maps* 12, 249–259.
- Ely C., J., Clark D., C., Hindmarsh C., R., Hughes L., A., Greenwood L., S., Bradley L., S., Gasson, E., Gregoire, L., Gandy, N., Stokes R., C., 2019. Recent progress on combining geomorphological and geochronological data with ice sheet modelling, demonstrated using the last British–Irish Ice Sheet. *J. Quat. Sci.* Early View. Early View.
- Ely, J.C., Clark, C.D., Ng, F., Spagnolo, M., 2017. Insights on the formation of longitudinal surface structures on ice sheets from analysis of their spacing, spatial distribution, and relationship to ice thickness and flow. *J. Geophys. Res.: Earth Surf.* 122, 961–972.
- Evans, D.J.A., 2017. Regional drainage history and long term landscape evolution. In: Evans, D.J.A. (Ed.), *The Quaternary Landscape History of Teesdale and the North Pennines*. Field Guide. Quaternary Research Association, London, pp. 26–31.
- Evans, D.J.A., Bateman, M.D., Roberts, D.H., Medialdea, A., Hayes, L., Duller, G.A., Fabel, D., Clark, C.D., 2017a. Glacial Lake Pickering: stratigraphy and chronology of a proglacial lake dammed by the North Sea Lobe of the British–Irish ice sheet. *J. Quat. Sci.* 32, 295–310.
- Evans, D.J.A., Clark, C.D., Mitchell, W.A., 2005. The last British Ice Sheet: a review of the evidence utilised in the compilation of the Glacial Map of Britain. *Earth Sci. Rev.* 70, 253–312.
- Evans, D.J.A., Clark, C.D., Rea, B.R., 2008. Landform and sediment imprints of fast glacier flow in the southwest Laurentide Ice Sheet. *J. Quat. Sci.* 23, 249–272.
- Evans, D.J.A., Dinnage, M., Roberts, D.H., 2017b. Glaciation of the northern Pennines. In: Evans, D.J.A. (Ed.), *The Quaternary Landscape History of Teesdale and the North Pennines*. Field Guide. Quaternary Research Association, London, pp. 26–31.
- Evans, D.J.A., Dinnage, M., Roberts, D.H., 2018. Glacial geomorphology of Teesdale, northern Pennines, England: implications for upland styles of ice stream operation and deglaciation in the British–Irish Ice Sheet. *Proc. Geologists' Assoc.* 129, 697–735.
- Evans, D.J.A., Jamieson, S.S.R., 2017. The North Pennines climate and glacierisation: plateau icefields and the concept of average glaciation. In: Evans, D.J.A. (Ed.), *The Quaternary Landscape History of Teesdale and the North Pennines* - Field Guide. Quaternary Research Association, London, pp. 68–75.
- Evans, D.J.A., Livingstone, S.J., Vieli, A., Ó Cofaigh, C., 2009. The palaeoglaciology of the central sector of the British and Irish Ice Sheet: reconciling glacial geomorphology and preliminary ice sheet modelling. *Quat. Sci. Rev.* 28, 739–757.
- Evans, D.J.A., Thomson, S.A., 2010. Glacial sediments and landforms of Holderness, eastern England: a glacial depositional model for the North Sea Lobe of the British–Irish ice sheet. *Earth Sci. Rev.* 101, 147–189.
- Evans, D.J.A., Young, N.J.P., Ó Cofaigh, C., 2014. Glacial geomorphology of terrestrial-terminating fast flow lobes/ice stream margins in the southwest Laurentide Ice Sheet. *Geomorphology* 204, 86–113.
- Fabel, D., Ballantyne, C.K., Xu, S., 2012. Trilines, blockfields, mountain-top erratics and the vertical dimensions of the last British–Irish Ice Sheet in NW Scotland. *Quat. Sci. Rev.* 55, 91–102.
- Fairburn, W.A., Bateman, M.D., 2016. A new multi-stage recession model for Proglacial Lake Humber during the retreat of the last British–Irish Ice Sheet. *Boreas* 45, 133–151.
- Finlayson, A., Merritt, J., Browne, M., Merritt, J., McMillan, A., Whitbread, K., 2010. Ice sheet advance, dynamics, and decay configurations: evidence from west central Scotland. *Quat. Sci. Rev.* 29, 969–988.
- Friend, R., Buckland, P., Friend, R., Buckland, P., Bateman, M., Panagiotakopulu, E., 2016. The 'Lindholme advance' and the extent of the last glacial maximum in the Vale of York. *Mercian Geol.* 19, 18–25.
- Gaunt, G.D., 1974. A radiocarbon date relating to Lake Humber. *Proc. Yorks. Geol. Soc.* 40, 195–197.
- Gaunt, G., 1975. The Devensian maximum ice limit in the Vale of York. *Proc. Yorks. Geol. Soc.* 40, 631–637.
- Glasser, N.F., Davies, B.J., Carrivick, J.L., Rodés, A., Hambrey, M.J., Smellie, J.L., Domack, E., 2014. Ice-stream initiation, duration and thinning on James Ross Island, northern Antarctic Peninsula. *Quat. Sci. Rev.* 86, 78–88.
- Glasser, N.F., Jansson, K.N., Harrison, S., Kleman, J., 2008. The glacial geomorphology and Pleistocene history of South America between 38°S and 56°S. *Quat. Sci. Rev.* 27, 365–390.
- Greenwood L., S., Clark D., C., 2009. Reconstructing the last Irish Ice Sheet 2: a geomorphologically-driven model of ice sheet growth, retreat and dynamics. *Quat. Sci. Rev.* 28, 3101–3123.
- Greenwood, S.L., Clark, C.D., Hughes, A.L.C., 2007. Formalising an inversion methodology for reconstructing ice-sheet retreat patterns from meltwater channels: applications to the British Ice Sheet. *J. Quat. Sci.* 22, 637–645.
- Hall, M., Cooper, A., Ford, J., Price, S., Burke, H., 2010. *The Use of NEXTMap Britain for Geological Surveying in the Vale of York*. Geological Society, London, pp. 55–66. Special Publications 345.
- Harmer, F.W., 1928. The distribution of erratics and drift. In: *Proceedings of the Yorkshire Geologists' and Polytechnic Society*, vol. 21, pp. 79–150.
- Hubbard, A., Bradwell, T., Colledge, N., Hall, A., Patton, H., Sugden, D., Cooper, R., Stoker, M., 2009. Dynamic cycles, ice streams and their impact on the extent, chronology and deglaciation of the British–Irish Ice Sheet. *Quat. Sci. Rev.* 28, 758–776.

- Huddart, D., 1981. Fluvio-glacial Systems in Edenside (Middle Eden Valley and Brampton Kame Belt). Quaternary Research Association, London, pp. 81–103.
- Huddart, D., Tooley, M., Carter, P., 1977. The Coasts of Northwest England, The Quaternary History of the Irish Sea. Seel House Press, Liverpool.
- Hughes, A.L.C., Greenwood, S.L., Clark, C.D., 2011. Dating constraints on the last British-Irish Ice Sheet: a map and database. *J. Maps* 7, 156–184.
- Hughes, A.L.C., Gyllencreutz, R., Lohne, Ø.S., Mangerud, J., Svendsen, J.I., 2016. The last Eurasian ice sheets—a chronological database and time-slice reconstruction, DATED-1. *Boreas* 45, 1–45.
- Hughes, A.L.C., 2008. The Last British Ice Sheet: a Reconstruction Based on Glacial Landforms, Geography, PhD Thesis. University of Sheffield, Sheffield, p. 307.
- Hughes, A.L.C., Clark, C.D., Jordan, C.J., 2010. Subglacial bedforms of the last British ice sheet. *J. Maps* 6, 543–563.
- Hughes, A.L.C., Clark, C.D., Jordan, C.J., 2014. Flow-pattern evolution of the last British ice sheet. *Quat. Sci. Rev.* 89, 148–168.
- Innes, J.B., Evans, D.J.A., 2017. Parrick House – a postglacial palaeoenvironmental archive. In: Evans, D.J.A. (Ed.), *The Quaternary Landscape History of Teesdale and the North Pennines*. Quaternary Research Association, London, pp. 186–193.
- Ivy-Ochs, S., Kober, F., 2007. Cosmogenic nuclides: a versatile tool for studying landscape change during the Quaternary. *Quat. Perspect.* 160, 134–138.
- Johnson, G.A.L., 1995. Robson's Geology of North East England, vol. 56. Transaction of the Natural History Society of Northumbria, Newcastle. Part 5.
- Joughin, I., Bindenschadler, R.A., King, M.A., Voigt, D., Alley, R.B., Anandakrishnan, S., Horgan, H., Peters, L., Winberry, P., Das, S.B., Catania, G., 2005. Continued deceleration of Whillans Ice Stream, west Antarctica. *Geophys. Res. Lett.* 32, L22501.
- Kelly, M.A., Lowell, T.V., Hall, B.L., Schaefer, J.M., Finkel, R.C., Goehring, B.M., Alley, R.B., Denton, G.H., 2008. A  $^{10}\text{Be}$  chronology of lateglacial and Holocene mountain glaciation in the Scoresby Sund region, east Greenland: implications for seasonality during lateglacial time. *Quat. Sci. Rev.* 27, 2273–2282.
- Kendall, P.F., Wroot, H.E., 1924. *Geology of Yorkshire*. Scholar Press, Menton.
- King, C.A.M., 1976. *The Geomorphology of the British Isles: Northern England*. Methuen, London.
- Kleman, J., Häfström, C., Stroeve, A.P., Jansson, K.N., De Angelis, H., Borgström, I., 2006. Reconstruction of Palaeo-Ice Sheets – Inversion of Their Glacial Geomorphological Record. *Glacier Science and Environmental Change*. Wiley Online Books.
- Krabbenam, M., Eyles, N., Putkinen, N., Bradwell, T., Arbelaez-Moreno, L., 2016. Streamlined hard beds formed by palaeo-ice streams: a review. *Sediment. Geol.* 338, 24–50.
- Linton, D.L., 1962. Glacial erosion on soft-rock outcrops in central Scotland. *Buletyn Peryglacjalny* 11, 247–257.
- Livingstone, S.J., Evans, D.J., Ó Cofaigh, C., Davies, B.J., Merritt, J.W., Huddart, D., Mitchell, W.A., Roberts, D.H., Yorke, L., 2012. Glaciodynamics of the central sector of the last British–Irish Ice Sheet in northern England. *Earth Sci. Rev.* 111, 25–55.
- Livingstone, S.J., Evans, D.J.A., Ó Cofaigh, C. (Eds.), 2010a. *The Quaternary of the Solway Lowlands and Pennine Escarpment*. Quaternary Research Association, Pontypool, South Wales, p. 154.
- Livingstone, S.J., Evans, D.J.A., Ó Cofaigh, C., 2010b. Re-advance of Scottish ice into the Solway lowlands (Cumbria, UK) during the main late Devensian deglaciation. *Quat. Sci. Rev.* 29, 2544–2570.
- Livingstone, S.J., Evans, D.J.A., Ó Cofaigh, C., Hopkins, J., 2010c. The Brampton Kame Belt and Pennine escarpment meltwater channel system (Cumbria, UK): morphology, sedimentology and formation. *Proc. Geologists' Assoc.* 121, 423–443.
- Livingstone, S.J., Ó Cofaigh, C., Evans, D.J.A., 2010d. A major ice drainage outlet of the last British-Irish Ice Sheet: the Tyne Gap, northern England. *J. Quat. Sci.* 25, 354–370.
- Livingstone, S.J., Ó Cofaigh, C., Evans, D.J.A., Palmer, A., 2010e. Sedimentary evidence for a major glacial oscillation and proglacial lake formation in the Solway Lowlands (Cumbria, UK) during Late Devensian deglaciation. *Boreas* 39, 505–527.
- Livingstone, S.J., Evans, D.J.A., Roberts, D.H., Davies, B.J., Ó Cofaigh, C., 2017. Glacial landforms and chronology of the Stainmore palaeo-ice stream on Cotherstone Moor. In: Evans, D.J.A. (Ed.), *The Quaternary Landscape History of Teesdale and the North Pennines*. Quaternary Research Association, London, pp. 194–199.
- Livingstone, S.J., Ó Cofaigh, C., Evans, D.J.A., 2008. Glacial geomorphology of the central sector of the last British-Irish Ice Sheet. *J. Maps* 2008, 358–377.
- Livingstone, S.J., Roberts, D.H., Davies, B.J., Evans, D.J.A., Ó Cofaigh, C., Gheorghiu, D.M., 2015. Late Devensian deglaciation of the Tyne Gap palaeo-ice stream, northern England. *J. Quat. Sci.* 30, 790–804.
- Lovell, H., Livingstone, S.J., Boston, C.M., Booth, A.D., Storrar, R.D., Barr, I.D., 2019. Complex kame belt morphology, stratigraphy and architecture. *Earth Surf. Process. Landforms*.
- Manley, G., 1961. The late-glacial climate of north-west England. *Geol. J.* 2, 188–215.
- Margold, M., Stokes, C.R., Clark, C.D., 2015. Ice streams in the Laurentide Ice Sheet: identification, characteristics and comparison to modern ice sheets. *Earth Sci. Rev.* 143, 117–146.
- McCabe, M., Knight, J., McCarron, S., 1998. Evidence for Heinrich event 1 in the British Isles. *J. Quat. Sci.* 13, 549–568.
- McCarroll, D., Stone, O., Ballantyne, K., C., Scourse, D., J., Fifield, K., L., Evans, J.A., D., Hiemstra, F., J., 2010. Exposure-age constraints on the extent, timing and rate of retreat of the last Irish Sea ice stream. *Quat. Sci. Rev.* 29, 1844–1852.
- McMillan, A.A., Hamblin, R.J.O., Merritt, J.W., 2011. A Lithostratigraphical Framework for Onshore Quaternary and Neogene (Tertiary) and Offshore Quaternary and Neogene (Tertiary) Superficial Deposits of Great Britain and the Isle of Man. British Geological Survey Research Report RR/10/03, p. 343.
- Mills, D.A.C., Hull, J.H., 1976. *Geology of the Country Around Barnard Castle*. Memoir of the Geological Survey of Great Britain. HMSO, London.
- Mitchell, W.A., 1994. Drumlins in ice sheet reconstructions with reference to the western Pennines, northern England. *Sediment. Geol.* 91, 313–331.
- Mitchell, W.A., 1996. Significance of snowblow in the generation of Loch Lomond Stadial (younger Dryas) glaciers in the western Pennines, northern England. *J. Quat. Sci.* 11, 233–248.
- Mitchell, W.A., Bridgland, D.R., Innes, J.B., 2010. Late Quaternary evolution of the Tees–Swale interfluve east of the Pennines: the role of glaciation in the development of river systems in northern England. *Proc. Geologists' Assoc.* 121, 410–422.
- Mitchell, W.A., Riley, J.M., 2006. Drumlin map of the western Pennines and southern Vale of Eden, northern England. *J. Maps* 10–16.
- Murton, D.K., 2018. A re-evaluation of late Devensian Glacial lake Humber levels in the Vale of York, UK. *Proc. Geologists' Assoc.* 129, 561–576.
- Murton, D.K., Murton, J.B., 2012. Middle and Late Pleistocene glacial lakes of low-land Britain and the southern North Sea basin. *Quat. Int.* 260, 115–142.
- Murton, D.K., Pawley, S.M., Murton, J.B., 2009. Sedimentology and luminescence ages of Glacial Lake Humber deposits in the central Vale of York. *Proc. Geologists' Assoc.* 120, 209–222.
- Ó Cofaigh, C., Evans, D.J.A., Smith, I.R., 2010. Large-scale reorganization and sedimentation of terrestrial ice streams during late Wisconsinan Laurentide Ice Sheet deglaciation. *GSA Bull.* 122, 743–756.
- Plater, A.J., Ridgway, J., Rayner, B., Shennan, I., Horton, B.P., Hayworth, E.Y., Wright, M.R., Rutherford, M.M., Wintle, A.G., 2000. Sediment provenance and flux in the Tees estuary: the record from the late Devensian to the present. In: Shennan, I., Andrews, J. (Eds.), *Holocene Land–Ocean Interaction and Environmental Change Around the North Sea*. Geological Society of London. Special Publications, London, pp. 171–195.
- Powers, M.C., 1953. A new roundness scale for sedimentary particles. *J. Sediment. Petrol.* 23, 117–119.
- Putnam, A.E., Schaefer, J.M., Barrell, D.J.A., Vandergoes, M., Denton, G.H., Kaplan, M.R., Finkel, R.C., Schwartz, R., Goehring, B.M., Kelley, S.E., 2010. In situ cosmogenic  $^{10}\text{Be}$  production-rate calibration from the Southern Alps, New Zealand. *Quat. Geochronol.* 5, 392–409.
- Rignot, E., Mouginot, J., Scheuchl, B., 2011. Ice flow of the Antarctic ice sheet. *Science* 333, 1427–1430.
- Roberts, D.H., Evans, D.J.A., Callard, S.L., Clark, C.D., Bateman, M.D., Medialdea, A., Dove, D., Cotterill, C.J., Saher, M., Ó Cofaigh, C., Chiverrell, R.C., Moreton, S.G., Fabel, D., Bradwell, T., 2018a. Ice marginal dynamics of the last British-Irish ice sheet in the southern North Sea: ice limits, timing and the influence of the Dogger Bank. *Quat. Sci. Rev.* 198, 181–207.
- Roberts, D.H., Grimoldi, E., Callard, L., Evans, D.J.A., Clark, C.D., Stewart, H.A., Dove, D., Saher, M., Ó Cofaigh, C., Chiverrell, R.C., 2018b. The mixed-bed glacial landform imprint of the North Sea Lobe in the western North Sea. *Earth Surf. Process. Landforms* 44, 1233–1258.
- Roberts, D.H., Long, A.J., Schnabel, C., Davies, B.J., Xu, S., Simpson, M.J.R., Huybrechts, P., 2009. Ice sheet extent and early deglacial history of the southwestern sector of the Greenland Ice Sheet. *Quat. Sci. Rev.* 28, 2760–2773.
- Rose, J., Letzer, J.M., 1977. Superimposed drumlins. *J. Glaciol.* 18, 471–480.
- Siebert, M., Ross, N., Corr, H., Kingslake, J., Hindmarsh, R., 2013. Late Holocene ice-flow reconfiguration in the Weddell sea sector of West Antarctica. *Quat. Sci. Rev.* 78, 98–107.
- Siebert, M.J., Welch, B., Morse, D., Vieli, A., Blankenship, D.D., Joughin, I., King, E.C., Vieli, G., Payne, A.J., Jacobel, R., 2004. Ice flow direction change in interior West Antarctica. *Science* 305, 1948–1951.
- Small, D., Clark, C.D., Chiverrell, R.C., Smedley, R.K., Bateman, M.D., Duller, G.A.T., Ely, J.C., Fabel, D., Medialdea, A., Moreton, S.G., 2017. Devising quality assurance procedures for assessment of legacy geochronological data relating to deglaciation of the last British-Irish Ice Sheet. *Earth Sci. Rev.* 164, 232–250.
- Small, D., Fabel, D., 2015. A Lateglacial  $^{10}\text{Be}$  production rate from glacial lake shorelines in Scotland. *J. Quat. Sci.* 30, 509–513.
- Smith, M.J., Clark, C.D., 2005. Methods for the visualization of digital elevation models for landform mapping. *Earth Surf. Process. Landforms* 30, 885–900.
- Stoker, M., Bradwell, T., 2005. The Minch palaeo-ice stream, NW sector of the British-Irish Ice Sheet. *J. Geol. Soc. Lond.* 162, 425–428.
- Stokes, C.R., Clark, C.D., 2001. Palaeo-ice streams. *Quat. Sci. Rev.* 20, 1437–1457.
- Stokes, C.R., Tarasov, L., Blomdin, R., Cronin, T.M., Fisher, T.G., Gyllencreutz, R., Häfström, C., Heyman, J., Hindmarsh, R.C.A., Hughes, A.L.C., Jakobsson, M., Kirchner, N., Livingstone, S.J., Margold, M., Murton, J.B., Noormets, R., Peltier, W.R., Peteet, D.M., Piper, D.J.W., Preusser, F., Renssen, H., Roberts, D.H., Roche, D.M., Saint-Ange, F., Stroeve, A.P., Teller, J.T., 2015. On the reconstruction of palaeo-ice sheets: recent advances and future challenges. *Quat. Sci. Rev.* 125, 15–49.
- Stone, P., Millward, D., Young, B., Merritt, J.W., Clarke, S.M., McCormac, M., Lawrence, D.J.D., 2010. *British Regional Geology: Northern England*, fifth ed. British Geological Survey, HMSO, Keyworth, Nottingham.
- Straw, A., Clayton, K.M., 1979. Eastern and central England. In: *The Geomorphology of the British Isles*. Methuen, pp. 21–45.
- Trotter, S.E., Hollingworth, S.E., 1932. The glacial sequence in northern England. *Geol. Mag.* 69, 374–380.



- Wilson, P., Bentley, M.J., Schnabel, C., Clark, R., Xu, S., 2008. Stone run (block stream) formation in the Falkland Islands over several cold stages, deduced from cosmogenic isotope ( $^{10}\text{Be}$  and  $^{26}\text{Al}$ ) surface exposure dating. *J. Quat. Sci.* 23, 461–473.
- Wilson, P., Clark, R., 1995. Landforms associated with a Loch Lomond Stadial glacier at Cronkley scar, Teesdale, northern Pennines. In: *Proceedings of the Yorkshire Geological Society*, vol. 50, pp. 277–283.
- Wilson, P., Lord C., T., 2014. Towards a robust deglacial chronology for the northwest England sector of the last British-Irish Ice Sheet. *North West Geogr.* 14, 1–11.
- Wilson, P., Lord, T., Rodés, Á., 2013a. Deglaciation of the eastern Cumbria glaciokarst, northwest England, as determined by cosmogenic nuclide ( $^{10}\text{Be}$ ) surface exposure dating, and the pattern and significance of subsequent environmental changes. *Cave Karst Sci.* 40, 22–27.
- Wilson, P., Schnabel, C., Wilcken, K.M., Vincent, P.J., 2013b. Surface exposure dating ( $^{36}\text{Cl}$  and  $^{10}\text{Be}$ ) of post-Last Glacial Maximum valley moraines, Lake District, northwest England: some issues and implications. *J. Quat. Sci.* 28, 379–390.